Role of Pile Spacing on the Dynamic Behaviour of Pile Groups in Layered Soils

Thejesh Kumar Garala[1], PhD and Gopal S.P. Madabhushi[2], PhD

Abstract

This research investigates the influence of pile spacing on the dynamic behaviour of pile groups by performing a series of specifically designed dynamic centrifuge experiments on pile foundations embedded in a two-layered soil profile. A single pile and two 3 × 1 row pile groups with different pile spacing were used as model pile foundations, and the soil models consisted of a soft clay underlain by a dense sand. The influence of earthquake frequency on the dynamic behaviour of two-layered soils is discussed using the centrifuge data and 1D site response analysis from DEEPSOIL. Further, the results of these centrifuge tests agreed with the conviction that the group effects will be diminished with the increase in pile-to-pile spacing in a pile group due to reduced pile-soil-pile interaction. However, this reduced pile group effects can lead to larger kinematic pile bending moments in the widely spaced pile group compared to a closely spaced pile group. Moreover, the single pile always has larger bending moments than both the tested pile groups. An exception to this is when there is a significant phase difference between the kinematic and inertial loads for a single pile but not for the widely spaced pile group. The influence of pile spacing on the shadowing effects and location of peak bending moments in the piles of a group are also discussed. Lastly, an attempt is made to evaluate the individual contribution of inertial and kinematic loads for the seismic design of pile foundations considering soil-pile-structure interaction effects.

Key words: centrifuge, earthquakes, inertial load, kinematic load, pile group, pile spacing.

---

[1] (corresponding author) Research Fellow, Nottingham Centre for Geomechanics, University of Nottingham, UK and Former PhD Student, Schofield Centre, Department of Engineering, University of Cambridge, UK.
Email: thejeshgarala@gmail.com

[2] Professor of Civil Engineering & Director of Schofield Centre, Department of Engineering, University of Cambridge, UK.
Email: mspg1@cam.ac.uk

Introduction

During earthquakes, pile foundations will be subjected to lateral ground vibrations, referred to as kinematic loads, along with the vibrations induced by superstructure, called inertial loads. In the conventional seismic pile design, where mostly pseudo-static approaches are adopted, the pile foundations are designed only for inertial loads assuming the influence of kinematic loads is negligible compared to inertial loads. However, the studies of Mizuno (1985), Gazetas et al. (1993) and Nikolaou et al. (2001) highlight the significance of seismic kinematic loads and the potential damage caused by these loads to pile foundations at deeper levels where the inertial effects are negligible. Later, seismic design code for railway structures of Japan (RTRI 1999) and Eurocode 8 (CEN 2004) recommends considering the kinematic loads generated during earthquakes along with the inertial loads in the design of piles and piers. The pile foundations will be subjected to severe kinematic loads either due to the lateral spreading of liquefied soil or due to the kinematic interaction close to pile head in very soft soil and at the interface between two-layers of soil with significant stiffness contrast. The effects of lateral spreading have received a significant attention (e.g. Madabhushi et al. 2010), however, there is a scarcity of experimental research on kinematic interaction in a level ground (Garala et al. 2020).

Dobry and O'Rourke (1985), Nikolaou et al. (2001), Mylonakis (2001), Maiorano et al. (2009), Sica et al. (2011), Di Laora et al. (2012) and Ke et al. (2019), among others, studied the kinematic pile bending response at the interface of two-layered soils. These studies proposed equations for determining the peak kinematic pile bending moment using finite element methods or beam on dynamic Winkler foundation analyses, by treating the soil behaviour as either linear-elastic or visco-elastic. Recently, Garala et al. (2020) investigated the kinematic pile bending moments of a single pile and pile group in a layered soil for a wide range of earthquake intensities using dynamic centrifuge experiments. The study of Garala et al. (2020) emphasises the importance of considering soil non-linearity effects and accurate shear strains at the interface of soil layers for a reliable assessment of kinematic pile bending moment from the existing literature methods.

In field conditions, both the kinematic and inertial loads occur together and therefore, it is difficult to understand their individual role on the overall pile dynamic behaviour. The combined effect of kinematic and inertial loads on the seismic response of pile foundations embedded in non-liquefiable soil layers have been evaluated through finite element or finite difference numerical methods (Cai et al. 2000; Maheshwari et al. 2004; Chau et al. 2009; Luo et al. 2016; Wang et al. 2017), beam on Winkler foundation analysis (Mylonakis et al. 1997; Murono and Nishimura 2000; Shirato et al. 2008; Rovithis et al. 2009; Kampitsis et al. 2013; Rahmani et al. 2018), dynamic centrifuge experiments (Wilson 1998; Boulanger et al. 1999; Hussien et al. 2016; Yoo et al. 2017; Garala and Madabhushi 2020; Garala 2020) and 1*g* shaking table tests (Meymand 1998; Shirato et al. 2008; Pitilakis et al. 2008; Chau et al. 2009; Hokmabadi 2014; Durante et al. 2016). Nevertheless, very few studies focused on the phase relationship between the seismic kinematic and inertial loads for pile foundations as listed in Table 1.

The contradictory conclusions shown in Table 1 and the limited literature on the phase relationship between the seismic kinematic and inertial loads clearly indicate the complexity of the interaction problem. However, the phase relationship theory proposed by Garala and Madabhushi (2020) agrees well with the fundamental concepts of structural dynamics. According to Garala and Madabhushi (2020), the phase difference between the seismic kinematic and inertial loads follows the conventional phase variation between the force and displacement of a viscously damped simple oscillator excited by a harmonic force.

Despite the research on evaluating the dynamic behaviour of pile foundations from past few decades, the influence of pile spacing on the dynamic behaviour of pile groups is yet unclear. Based on numerical analyses, Fan et al. (1991) reveals that the configuration of pile group, number of piles and spacing between the piles in a group have insignificant effects on kinematic lateral displacements. However, it is important to understand the pile spacing effects on kinematic pile bending moments, especially for non-linear soil conditions during large intensity earthquakes. Further, group shadowing effects are investigated mostly from static or cyclic load tests by applying a horizontal load at pile head (e.g. Rollins et al. 2006). However, these shadowing effects may not be applicable for time varying earthquake loads. Also, the influence of phase difference between the kinematic and inertial loads on the dynamic behaviour of pile groups with different spacing is not fully explored. Therefore, there is a need to explore the role of pile spacing on the dynamic behaviour of pile groups in non-liquefiable, layered soils with emphasis on the individual effect of kinematic and inertial loads.

In this study, a series of dynamic centrifuge experiments was carried out at 60*g* on pile foundations embedded in a two-layered soil model to study the influence of pile spacing on the overall dynamic behaviour of pile groups. A model single pile and two 3×1 row pile groups with different spacing were tested under model earthquakes of different intensities and frequencies. The soil profile consisted of a soft kaolin clay overlying a dense, fraction-B Leighton Buzzard (LB) sand. Each centrifuge experiment was carried out in two-flights, with acrylic plexiglass as pile caps in flight-01 and pile caps made from brass in flight-02, to examine the individual effect of kinematic and inertial loads. This paper initially discusses the strength and stiffness of soil layers and the dynamic behaviour of two-layered soil strata. Later, the influence of pile spacing on pile group accelerations and pile bending moments was discussed during kinematic loads alone and in the presence of both kinematic and inertial loads. In the end, the individual contribution of kinematic and inertial loads on the seismic behaviour of tested pile foundations was evaluated by adopting some of the methods available in the literature.

Physical Modelling using the Centrifuge

Centrifuge modelling

Centrifuge modelling facilitates the scaling of geotechnical structures as small models, yet replicating the field stress-strain conditions by subjecting the models to increased *g*-field conditions. Due to the increased gravitational field in the centrifuge, the self-weight soil stresses in the scaled model substantially increase with depth and resemble full-scale soil stress profiles. More details related to the geotechnical centrifuge modelling can be found in Schofield (1980) and Madabhushi (2014). The centrifuge experiments performed in this research were conducted at 60*g* using the Turner beam centrifuge (Schofield 1980) facilities at the Schofield Centre, University of Cambridge. It is a 10 m diameter centrifuge which rotates about the central vertical axis with a working radius of 4.125 m. Further, an equivalent shear beam (ESB) box was used as a model container. The ESB box used in this study consists of nine rectangular higher aircraft grade aluminium hollow sections stacked together with the rubber in between. Brennan and Madabhushi (2002) presents the similar ESB box design and construction. These ESB containers minimise the reflected energy from boundary walls to simulate seismic energy radiating away into the field (Teymur and Madabhushi 2003). To simulate the model earthquakes in the centrifuge, servo-hydraulic earthquake actuator developed by Madabhushi et al. (2012) was used. This actuator is able to simulate the realistic earthquake motions along with the simple sinusoidal excitations of varying amplitudes and multiple frequency components.

Soil models and model pile foundations

In this series of centrifuge experiments, the soil models were prepared with a dense, poorly graded, fraction-B Leighton Buzzard (LB) sand underlying the soft speswhite kaolin clay to maintain significant stiffness contrast between the soil layers. The properties of fraction-B LB sand and speswhite kaolin clay can be found in Garala et al. (2020). For model pile foundations, a single pile (SP) and two 3×1 row pile groups were fabricated using an aluminium (Alloy 6061 T6) circular tube of outer diameter (d) 11.1 mm and thickness (t) 0.9 mm. BS 8004 (BSI 2015) recommends a minimum pile spacing of 3d centre-to-centre for the circular friction piles. Therefore, one of the pile groups was fabricated with 3d centre-to-centre spacing and the other pile group with a pile spacing of 5d centre-to-centre to investigate the pile spacing effects on the dynamic behaviour of pile groups. Hereafter, the 3d centre-to-centre spaced pile group will be referred as closely spaced pile group (CPG) and the 5d centre-to-centre spaced pile group as widely spaced pile group (WPG). The bottom of the tubular piles is closed with an aluminium plug to restrict the entry of soil into the piles during pile installation. Further, the single pile and end piles of the two pile groups (CPG and WPG) were strain gauged to measure the bending moments during earthquakes. Fig. 1 shows the schematic view of the pile foundations used in the study along with the location of strain gauges. The equivalent prototype characteristics of a single pile can be found in Garala and Madabhushi (2020).

Test suite

Two centrifuge experiments, namely Test-FPC and Test-FPW, were performed in this study. The relative density of sand in both the tests is around 85 ± 2% and consolidated clay layer has a saturated unit weight of 16.2 kN/m^3 and 16.4 kN/m^3 in Test-FPC and Test-FPW, respectively. The SP and CPG were tested in Test-FPC, while the WPG and the same SP as in Test-FPC were tested in Test-FPW. Fig. 2 shows the plan view of Test-FPW and Fig. 3 shows the elevation of the model along with the instrument locations in Test-FPW. The dimensions in Figs. 1 to 3 are at model scale, and the values within the parentheses represent the prototype dimensions. As shown in Fig. 3, the pile caps for foundations were placed at 20 mm (at model scale) above the soil surface. The detailed model preparation, plan view and elevation of the centrifuge model for Test-FPC can be found in Garala et al. (2020) and Garala and Madabhushi (2020). Piezoelectric accelerometers (PAs) were used to measure the accelerations in the soil model and micro-electro-mechanical systems accelerometers (MEMSs) were used to measure both horizontal and vertical accelerations in the pile foundations during the model earthquakes, as shown in Fig. 3. The response from the piezoelectric accelerometers can be considered as the far-field soil response as they were placed at a distance greater than 10*d* from either end of the pile foundations and in a different vertical plane, as shown in Fig. 2. Linear variable displacement transducers (LVDTs) were used to measure the displacements of soil surface and pile foundations in both tests.

Further, each centrifuge experiment was carried out in two-flights, with acrylic plexiglass as pile caps in flight-01 and pile caps made from brass in flight-02, to examine the individual effect of kinematic and inertial loads. Mass of the plexiglass caps for single pile, closely spaced and widely spaced pile groups are 11 g, 24 g and 33 g, respectively, at model scale. These masses are less than half the self-weight of the pile foundations (each model pile weighs 24 g without strain gauges) and negligible in comparison to the axial load carrying capacity of the single pile (0.57 kg at model scale). Hence, the pile accelerations and bending moments measured during the flight-01 can be considered as the effect of kinematic loads alone on the pile foundations. In flight-02 of each centrifuge test, the brass caps will induce a static vertical force of 167.75 N and 503.25 N at model scale (0.604 MN and 1.812 MN at prototype scale) for single pile and pile groups, respectively, thereby vertical load acting per pile is same for both single pile and pile groups. The applied vertical load is half the axial load carrying capacity of the pile foundations. Therefore, the pile accelerations and bending moments measured in flight-02 are due to the combined effect of both kinematic and inertial loads. In the following sections, flight-01 and flight-02 are referred as ‘K’ and ‘K+I’ flights, respectively.

Model earthquakes and data processing

Fig. 4 shows the acceleration time-histories and corresponding fast Fourier transforms (FFTs) of earthquakes (here after called as base excitations (BEs)) considered in this study. As shown in Fig. 4, BE1 to BE4 excitations have 10 cycles of sinusoidal loading with different frequencies, BE5 is a scaled 1995 Kobe earthquake motion and BE6 is a sine-sweep excitation with prototype frequencies ranging from 0.3 Hz to 2.5 Hz. The excitations considered enable to investigate the effect of kinematic and inertial loads on the pile foundations for a variety of shaking intensities and frequencies. In terms of centrifuge data processing, the electrical devices and earthquake actuator might induce noises and interfere with the data obtained from instruments in the dynamic centrifuge experiments (Madabhushi 2014). To this end, the raw centrifuge data was filtered using a low-pass 4th order Butterworth filter with a cut-off prototype frequency of 5 Hz in most cases. While integrating the accelerations to obtain displacements, the data was also filtered using a high-pass 4th order Butterworth filter with a cut-off prototype frequency of 0.1 Hz to eliminate the signal drifting due to low frequency noise in the signals. The natural frequencies of tested soil models and soil-pile systems will be ranging from 0.6 Hz to 2 Hz, at prototype scale. Therefore, the chosen cut-off frequencies will ensure the non-removal of any useful frequency component, including the higher harmonics, from the measured seismic response of soil and pile foundations. The outcomes from these series of centrifuge experiments are discussed in the following sections, in which all the experimental data is presented at prototype scale unless stated otherwise.

Strength and Stiffness of the Soil Layers

The undrained shear strength (c_u) of the clay layer before subjecting the model to base excitations was evaluated by performing the in-flight T-bar tests (Garala et al. 2020) at 60*g* during K flight of both centrifuge tests. Fig. 5a shows the c_u profile of the clay layer in both tests. Further, an air hammer device (Ghosh and Madabhushi 2002) was used to determine the shear wave velocity (v_s) at different depths of soil model before firing the base excitations in both flights and in both centrifuge tests. From the measured v_s, the maximum shear modulus (G_0) was computed using Eq. 1. Figs. 5b and 5c show the G_0 profile of soil model in both flights during Test-FPC and Test-FPW, respectively.

$$G_0 = \rho v_s^2 \tag{1}$$

where ρ is the mass density of the corresponding soil layer.

Figs. 5b and 5c also show the G_0 of soil layers computed from Hardin and Drnevich (1972), Viggiani and Atkinson (1995) and Oztoprak and Bolton (2013). The equations used to compute the G_0 of soil layers from the literature methods can be seen in Garala et al. (2020). As Figs. 5b and 5c depicts, the G_0 values obtained from the air-hammer device are reasonably in good agreement with the G_0 evaluated from literature methods in both tests. To calculate the average stiffness contrast between the soil layers, the G_0 values at a depth of 4d–5d above and below the interface are considered as the average G_0 for the clay and sand layers, respectively. By considering the average shear modulus values for the soil layers as shown in Figs. 5b and 5c, there will be a stiffness contrast of about eight and ten between the clay and sand layers in Test-FPC and Test-FPW, respectively.

Though the model preparation is same for both Test-FPC and Test-FPW, the considerable difference in c_u and G_0 profiles for the clay layer is due to the different suctions in the clay layer before spinning in the centrifuge. After consolidating the clay slurry at 1*g*, the model will be unloaded from consolidometer by maintaining a suction of -60 kPa to -70 kPa in the clay layer (see Garala et al. 2020 for more details about the clay layer preparation). This suction continues to drop at a very slow rate by extracting water either from the bottom saturated sand layer or the moisture from atmosphere. Though the plan is to test the centrifuge models as early as possible after unloading from the consolidometer, there will be some delays in placing the instruments or testing in the centrifuge. Therefore, the net suction in the clay layers will not be the same in all centrifuge tests and hence the effective stresses will be different in different centrifuge tests, leading to slightly different c_u and G_0 profiles. However, having a prior information on c_u and G_0 profiles will assist in comparing the results from different centrifuge tests by normalising the data with appropriate parameters. This will be discussed in detail in the later sections.

Natural Frequencies of Soil Strata and Pile Foundations

The main intention behind the adoption of smaller intensity sine-sweep excitation (BE6) with the frequencies ranging between 0.3 Hz to 2.5 Hz is to determine the natural frequencies of soil strata and soil-pile systems. However, due to some manual errors in its execution, BE6 excitation was not successfully fired by the servo-hydraulic shaker during K flight of Test-FPC. Therefore, scaled 1995 Kobe motion (BE5) was used to determine the natural frequencies during K flight of Test-FPC as it consists of a larger range of frequencies in comparison to simple sinusoidal excitations as shown in Fig. 4. BE6 excitation was used in all other cases. The natural frequencies of soil strata and soil-pile systems were determined by dividing the FFT of the soil surface acceleration and the pile-head acceleration, respectively with the FFT of base-excitation, referred to as transfer functions.

Figs. 6a-6d show the transfer functions computed from both flights of Test-FPC and Test-FPW. As it shows in Figs. 6a and 6c, both the single pile and pile groups are forced to follow the soil movement in the absence of vertical loads at the pile cap level. Slightly larger acceleration amplitude for the pile foundations in comparison to soil surface during K flights is due to the higher mass density of the pile material and corresponding inertial effects. Also, the single pile has higher acceleration amplitude than both the pile groups in K flight, probably due to the higher rotational stiffness of the pile groups compared to a single pile. Further, as expected, the pile foundations are vibrating at their own soil-pile system natural frequencies in the presence of vertical loads (K+I flight) as shown in Figs. 6b and 6d. The discrepancy in the natural frequency of soil strata in K flight (determined by using larger intensity Kobe motion) and K+I flight (determined by using smaller intensity sine-sweep excitation) during Test-FPC is probably due to the difference in shear strains induced by the corresponding base excitations.

Further, the natural frequency of soil strata in Test-FPW (1.7 Hz) is slightly smaller than the soil strata in Test-FPC (2.0 Hz). The single pile in Test-FPC has a natural frequency of 0.6 Hz in K+I flight (see Fig. 6b) but possess a slightly higher natural frequency of 0.78 Hz in K+I flight of test Test-FPW (see Fig. 6d). This difference in natural frequencies of the soil strata and same single pile tested in two different centrifuge tests can be due to the small differences in soil properties between the two tests, as shown in Fig. 5. Moreover, as shown in Figs. 6b and 6d, both the pile groups (CPG and WPG) have higher amplification ratios than the single pile in K+I flight. The probable reason for this might be the close proximity of natural frequencies of soil-strata and soil-pile group-structure systems, leading to double resonance conditions in the tested pile groups in K+I flight. The normalisation of transfer functions of the pile foundations with the response of soil-strata will indicate the true seismic behaviour of single pile and pile groups. Fig. 7 shows the normalised response of pile foundations in K+I flight of both tests. As Fig. 7 illustrates, the single pile can have higher normalised acceleration amplitude than both the pile groups due to the relatively lower rotational stiffness of the single pile compared to a pile group. In addition, though Figs. 6b and 6d indicate that the closely spaced and widely spaced pile groups possess the same natural frequency in K+I flight (~ 1.7 Hz), Fig. 7 clearly indicates that the widely spaced pile group can have a higher natural frequency compared to a closely spaced pile group. This is to be expected as the pile-soil-pile interaction will reduce with the increase in pile-to-pile spacing in a pile group, leading to a lower stiffness for closely spaced pile group compared to a widely spaced pile group.

Dynamic Response of Soil Strata

Figs. 8a and 8c show the peak acceleration measured at different depths of soil strata during all base excitations (BE1 to BE5) in both centrifuge tests. Also, the peak soil displacement at different depths is determined by double integrating the measured soil accelerations and shown in Figs. 8b and 8d. The shear wave amplification as it propagates from dense sand layer to the surface of soft clay layer can be clearly seen in Figs. 8a-8d. As it can be expected, due to the larger intensity of BE2 excitation (PBA = 0.087*g*) compared to BE1 excitation (PBA = 0.046*g*), the peak soil acceleration at all depths is always higher for BE2 excitation in comparison with BE1 excitation. However, the relatively higher frequency shear waves induced by BE2 excitation (1.167 Hz) have caused smaller displacements in the sand layer compared to the lower frequency BE1 excitation (0.667 Hz). This is due to the inverse relationship between the frequency of wave and its displacement. Nevertheless, the higher frequency shear waves cannot propagate quickly in the soft clay layer due to its lower shear wave velocities. To keep the energy (flux) of the wave constant, the higher frequency shear waves have caused a significant displacement in the clay layer compared to the lower frequency shear waves as shown in Figs. 8b and 8d. This difference in displacements in both the sand and clay layers can be larger when the intensities of BE1 and BE2 excitations are nearby. Similar behaviour was observed even between BE3 and BE4 excitations, which have nearby excitation intensities (PBAs of 0.174*g* and 0.193*g*, respectively) but different excitation frequencies (0.667 Hz and 0.83 Hz, respectively).

In Figs. 8a-8d, the peak amplification in the soil strata, in terms of both acceleration and displacement, can be observed during BE2 excitation. This is probably due to its predominant excitation frequency (1.167 Hz) being close to the strain-dependent natural frequency of the soil strata. Further, the shear strain values just above and beneath the interface of soil layers are determined for the peak acceleration cycles of sinusoidal base excitations (BE1 to BE4 excitations), following the methodology suggested by Brennan et al. (2005). Tables 2 and 3 show these shear strain values for Test-FPC and Test-FPW, respectively. As it shows in Tables 2 and 3, there is a significant strain contrast between the soil layers at higher frequencies (BE2 and BE4 excitations) compared to the relatively smaller frequency BE1 and BE3 excitations.

In addition, the seismic response of soil strata from centrifuge tests is compared with the one-dimensional seismic ground response analysis from DEEPSOIL (Hashash et al. 2017). For DEEPSOIL analysis, the soil strata was divided into a finite number of small layers, ensuring that the maximum frequency propagated by each layer is always greater than 30 Hz, as recommended by Hashash et al. (2017). Further, the thickness of discretised soil layers (t_s) was always less than 1/8th of the shortest wavelength of the base excitations considered in this study (see Eq. 2).

$$t_s < v_{s,min}/(8\times f_{max}) \qquad (2)$$

where $v_{s,min}$ is the minimum shear wave velocity and f_{max} is the maximum frequency component of base excitation (~5 Hz, as frequencies higher than this are filtered out in the centrifuge data processing).

The soil properties (density, shear wave velocity and undrained shear strength) in K flight of Test-FPC (see Figs. 5a and 5b) were assigned to each layer. For the sand layer, the shear strength was computed from the known properties of sand (mass density and friction angle) by adopting the standard Mohr-Coulomb equation. Further, the bedrock was assumed as rigid in this analysis. Garala et al. (2020) has shown that the shear modulus values determined during different base excitations for the soil strata in Test-FPC agrees well with the Darendeli (2001) modulus reduction curves, especially for the soft clay layer. In addition, Garala and Madabhushi (2019) highlighted the importance of performing non-linear seismic ground response analysis by accounting c_u in the analysis for the sites with soft clays. Therefore, non-linear analyses were performed in DEEPSOIL with the Darendeli (2001) modulus reduction and damping curves for both soft clay and sand layers. The two existing soil models, pressure-dependent modified Kondner Zelasko (MKZ model) and general quadratic/hyperbolic (GQ/H model), were used to check if these soil models in DEEPSOIL can simulate the two-layered soil response observed in the centrifuge tests. The GQ/H model facilitates the shear strength consideration by automatically adjusting the reference shear modulus and damping curves based on the specified shear strength at the large strains (Hashash et al. 2017), nevertheless, there is no such criteria in the MKZ model.

Figs. 9a to 9d show the comparison of soil strata response from K flight of Test-FPC and DEEPSOIL analyses. As it shows in Figs 9a and 9c, both the soil models considered in DEEPSOIL are well predicting the peak accelerations in soil strata during the smaller intensity excitations (BE1 and BE2 excitations), with values being very close to those observed in centrifuge test. However, both the soil models were suggesting the attenuation of accelerations at shallower depths during larger intensity excitations (BE3, BE4 and BE5 excitations), though there is no such behaviour in centrifuge tests.

In addition, the peak soil displacements from DEEPSOIL analyses are differing from the centrifuge data, especially in the clay layer (see Figs. 9b and 9d). This is valid even for BE2 excitation where the soil accelerations from DEEPSOIL are well matched with the centrifuge data. Further, both the soil models are unable to simulate the frequency effects observed on shear wave displacements in the layered soil during larger intensity excitations (BE3 and BE4 excitations). This might be troublesome when such erroneous ground response analyses are used to estimate the free-field soil displacements, for example in seismic kinematic soil-pile interaction problems, where it is usually assumed that the pile will follow the surrounding soil displacements (see Margason and Halloway 1977). It must be considered that the pile may not necessarily follow the surrounding soil motion during earthquakes, especially when there is a significant stiffness contrast between the pile and surrounding soil.

Nevertheless, the inaccurate free-field soil displacements can lead to erroneous determination of kinematic forces and can critically influence the overall kinematic response of pile foundations.

One of the possible reasons for the mismatch in displacements from the centrifuge data and DEEPSOIL analysis can be that the experimental displacement values were obtained by the double integration of measured acceleration time-histories. Therefore, the filtering techniques adopted in the data processing might have influenced the derived displacements to some extent. A further investigation is required to this end. In addition, Darendeli (2001) damping curves were used in the DEEPSOIL analysis, though its validity to the tested soil strata is not verified. Therefore, a thorough study is required investigating the applicability of damping curves proposed by Darendeli (2001) for the soil strata used in this series of centrifuge tests.

Dynamic Response of Pile Foundations

Fig. 10 shows the acceleration response of soil surface and tested pile foundations in both the flights. In Fig. 10, the soil surface and single pile accelerations from Test-FPC are only shown, as their overall dynamic behaviour is similar in both centrifuge tests with exception in acceleration magnitudes due to the different natural frequencies of soil strata and soil-single pile system (see Fig. 6). As Fig. 10 depicts, the soil surface accelerations are in-phase in both the flights during most base excitations, except some small difference during BE4 and BE5 excitations. However, there is a phase difference between K flight and K+I flight pile accelerations, especially in the single pile. Wang et al. (2017) suggests that the phase difference between the kinematic and inertial loads depends on the pile configuration by performing three-dimensional finite element simulations. To verify this suggestion, the phase difference between the kinematic and inertial loads is computed from the experimentally measured pile accelerations in both flights. Due to the negligible kinematic effects at the pile-cap level, the pile accelerations at the cap level are greatly influenced by the inertial loads in K+I flight. Therefore, the phase difference between the pile accelerations of K flight and K+I flight can be considered as the phase difference between the kinematic and inertial loads.

The phase difference between the K flight and K+I flight accelerations for all the tested pile foundations during different base excitations were determined using cross-power spectral density functions (see Garala and Madabhushi, 2020). Further, the predominant soil-pile-structure frequencies (f_{sps}) at which the peak acceleration amplification occur were determined for all the pile foundations during all base excitations in K+I flight, following the same procedure as natural frequencies determination (see Fig. 6). Experimentally determined phase difference values are plotted against the normalised frequency, f/f_{sps} (f is base-excitation frequency, see Fig. 4) and shown in Fig. 11. Fig. 11 also shows the variation of phase between the force and displacement of a viscously damped linear second-order system subjected to a harmonic response due to base acceleration or displacement for various damping ratios (ζ). As Fig. 11 shows, the phase difference between the kinematic and inertial loads for various f/f_{sps} ratios well agrees with the conventional force-displacement phase variation of a simple oscillator excited by a harmonic force for both single pile and pile groups with different spacing.

Further, the single pile has lower pile accelerations in K+I flight compared to K flight during BE2, BE4 and BE5 excitations (see Fig. 10) as there is a significant phase difference between the kinematic and inertial loads as shown in Fig. 11 (see Garala and Madabhushi 2020 for more details). Similarly, due to the smaller phase difference between the kinematic and inertial loads for pile groups during all base excitations (see Fig. 11), the accelerations of pile groups in K+I flight are always larger than K flight (see Fig. 10). In addition, the widely spaced pile group has smaller accelerations than closely spaced pile group during most base excitations. This can be due to the higher damping exhibited by the widely spaced pile group in comparison to closely spaced pile group as shown in Fig. 11, where most data points related to widely spaced pile group are in between ζ of 0.10 and 0.25, whereas for closely spaced pile group they are in between ζ of 0.05 and 0.10. The widely spaced pile group has larger accelerations at BE2 excitation compared to closely spaced pile group, as widely spaced pile group is responding at its nearby resonance conditions (f/f_{sps} close to 1) and exhibiting smaller damping during BE2 excitation (see Fig. 11). However, the accurate damping exhibited by the soil-pile systems cannot be directly interpreted from Fig. 11 as the theoretical equations are developed for linear systems, whereas the problem under investigation can induce higher non-linearity during larger intensity excitations. The slightly scattered data points for BE4 and BE5 excitations is probably due to the phase difference created by the mismatch in soil response in K flight and K+I flight (see Fig. 10). Therefore, the response from widely spaced pile group will add further evidence to the conclusion of Garala and

Madabhushi (2020) that the ratio of free-field soil natural frequency to the natural frequency of structure may not necessarily govern the phase relationship between the kinematic and inertial loads as reported by some studies in Table 1. Further, the phase relationship obtained in this study is also independent of pile configuration, opposing the conclusion of Wang et al. (2017). However, it is to be noted that though Fig. 11 is independent of soil natural frequency, the excitation frequencies considered in this study are smaller than the natural frequency of soil-strata.

Comparison of Kinematic Pile Bending Moments

Bending moments measured by the strain gauges on pile foundations (see Fig. 1) during the base excitations of K flight were used to compare the kinematic pile bending moments in single pile and pile groups. The bottom most gauge in the single pile (at a depth of 16.5 m in Fig. 1) did not work in Test-FPC and hence the bending moment values at this depth are not shown in the corresponding figures of following discussion. Further, the bending at pile tip is assumed to be zero for both single pile and end piles of the pile groups in both K flight and K+I flight.

It is essential to normalise the kinematic pile bending moments for a valid comparison among base excitations with different excitation intensities and frequencies. Kavvadas and Gazetas (1993) used Eq. 3 to normalise the pile bending moments, which was used later in several other studies (e.g. Hussien et al. 2016).

$$\widehat{M} = \frac{M}{\rho_p d^4 \ddot{u}_B} \tag{3}$$

where $\widehat{M}$ is the normalised bending moment, M is the bending moment, ρ_p is the mass density of the pile material, and $\ddot{u}_B$ is the amplitude of bedrock-acceleration.

However, Eq. 3 is proposed for linear analysis with deformation and stress quantities are being proportional to the bedrock excitation intensity, which will not be the case during larger intensity earthquakes that impose high soil non-linearity. Therefore, Eq. 4 is used in this study to normalise the kinematic pile bending moments. Eq. 4 considers the base excitation intensity, dynamic behaviour of free-field soil, dimensions of the pile section and characteristics of the pile material through pile flexural rigidity ($E_p I_p$). Further, the depth (z) of the soil is also normalised with the pile diameter (d) and presented as normalised soil depth (z/d) in this section.

$$M_{K\_Norm} = \frac{M_k}{\left(\frac{E_p I_p}{d}\right)\left(\frac{a_{sur\_peak}}{a_{base\_peak}}\right)\left(\frac{a_{base\_peak}}{g}\right)} = \frac{M_k}{\left(\frac{E_p I_p}{d}\right)\left(\frac{a_{sur\_peak}}{g}\right)} \tag{4}$$

where M_{K_Norm} is the normalised kinematic pile bending moment, M_k is the measured kinematic pile bending moment, a_{base_peak} and a_{sur_peak} are the peak base excitation and soil surface accelerations, respectively for the corresponding base excitation (see Figs. 4 and 10).

The kinematic pile bending moments in layered soils will greatly depend on the soil characteristics and stiffness contrast between the soil layers. As the soil strata characteristics are slightly different in Test-FPC and Test-FPW (see Figs. 5 and 8), the kinematic bending moments measured by the piles in pile groups (CPG and WPG) in two different tests are compared with the corresponding single pile tested in the same soil model. Figs. 12 and 13 show the normalised absolute maximum kinematic pile bending moments of closely spaced and widely spaced pile groups, respectively along with the single pile tested in corresponding tests. As shown in Figs. 12 and 13, the peak kinematic pile bending moment always occurs slightly beneath the interface of soil layers for single pile and pile groups with different pile spacing, irrespective of intensity of the excitation. This is due to the strain discontinuity between the soil layers of sharp stiffness contrast (see Tables 2 and 3). For a closely spaced pile group, the piles in the group are always subjected to the lower peak kinematic bending moments than the single pile and this difference increases with the increase in intensity of the excitation (see Fig. 12). Further, due to the shadowing effects, the end-piles of the closely spaced pile group (pile-1 and pile-3) are not subjected to the same peak kinematic pile bending moment. The influence of shadowing effects is significant at larger intensity earthquakes. In addition, the kinematic pile bending moment at a normalised soil depth of 14.2 is close to the value at a depth of 16.5 for the end piles in closely spaced pile group. This indicates that the peak kinematic pile bending moment occurs at a deeper location for the closely spaced pile group in comparison to a single pile. More discussion related to the kinematic pile bending response of single pile and closely spaced pile group can be found in Garala et al. (2020).

On the other hand, for the widely spaced pile group, the shadowing effects are significant with pile-1 having larger peak kinematic bending moments than pile-3. However, from depths ~1*d* beneath the soil interface, pile-3 possess larger kinematic bending moments than pile-1 as shown in Fig. 13. Further observations from Fig. 13 include:

- The peak kinematic bending moment in pile-1 of the widely spaced pile group is very close to the peak kinematic bending moment measured by the single pile during all base excitations.
- In a widely spaced pile group, the peak kinematic bending moment in the piles of group occurs at the same depth as single pile.
- The peak kinematic bending moments at the ground surface level will be significantly larger for the pile groups in comparison to single pile due to the frame action of pile groups.
- The piles of widely spaced pile group will have a significantly larger kinematic bending moments compared to piles of the closely spaced pile group at depths close to the ground surface level, especially during the larger intensity earthquakes (see Figs. 12 and 13).

The different shadowing effects and peak kinematic pile bending moment locations in the closely spaced and widely spaced pile groups can be due to the soil confinement effects between the piles in a group. In a closely spaced pile group, the confined soil between the closely spaced piles can act as a block and vibrate in unison with the pile foundations during excitations. While in widely spaced pile group, the soil in between the widely spaced piles can respond more like free-field soil behaviour and can impose different kinematic loads in sand and clay layers. Therefore, in a widely spaced pile group, the pile-group effects will be minimised due to less pile-soil-pile interaction resulting in a peak kinematic bending moment close to that of a single pile.

Comparison of Inertial Pile Bending Moments

During K flight, the single pile and pile groups follow the soil movement and hence the kinematic pile bending moments can be normalised by considering the soil strata characteristics alone for the comparison. However, in K+I flight, there will be inertial loads along with the kinematic loads, which will make the pile foundations to respond at their own soil-pile system natural frequencies. These soil-pile system natural frequencies will be different for different pile configurations (single pile and pile groups), as shown in Figs. 6b and 6d. Therefore, for comparing the bending moments of pile groups with different spacing from two different experiments, the measured bending moments in K+I flight should be normalised considering both frequency effects and soil strata characteristics. In this process, the single pile bending moments from two different centrifuge tests (Test-FPC and Test-FPW) are normalised with different frequency functions until a similar normalised bending moment profiles are obtained. It must be noted that the single pile has different natural frequencies (see Figs. 6b and 6d) and soil strata possess different characteristics (see Figs. 5 and 8) in Test-FPC and Test-FPW. Therefore, a good similarity between the normalised bending response of single pile from two different tests represents the accuracy of normalisation scheme adopted. By trial and error method, the frequency function, $\chi^{1-\chi^{0.25}}$ (χ is the frequency ratio, see Eq. 5a) shown in Fig. 14, is used to normalise the pile bending moments. Fig. 15 shows the single pile bending response obtained by normalising the pile bending moments from two different tests using Eq. 5b. As Fig. 15 shows, there is a good similarity in bending response during most base excitations (except BE3), thereby indicating the accuracy of adopted frequency normalisation.

$$\chi = \frac{f}{f_{sps}} \tag{5a}$$

$$M_{F\_Norm} = \frac{M}{\left(\frac{E_p I_p}{d}\right)\left(\frac{a_{sur\_peak}}{g}\right)\left(\chi^{1-\chi^{0.25}}\right)} \tag{5b}$$

where M_{Norm} is the normalised bending moment and M is the measured bending moment in K+I flight.

Therefore, Eq. 5b can be used to compare the bending moments of pile foundations with different pile-soil system natural frequencies and embedded in different soil strata. Nevertheless, the frequency normalisation function is developed based on centrifuge models tested in this particular study and hence may need further verification.

Fig. 16 shows the comparison of normalised absolute maximum bending moments (using Eq. 5b) of single pile (from Test-FPC) and end piles (pile-1 and pile-3) of the two pile groups during different base excitations in K+I flight. As Fig. 16 shows, the peak bending moment will be at the shallower depths for single pile in the presence of both kinematic and inertial loads, whereas the peak bending moment can occur either at the ground level or at the interface of soil layers for the piles in both pile groups. The single pile has smaller peak bending moments during BE4 and BE5 excitations compared to BE3 excitation despite they are all having nearby base excitation intensities. This is due to the larger phase difference between the kinematic and inertial loads during BE4 and BE5 excitations in comparison with BE3 excitation (see Fig. 11).

Further, the free-head condition of the single pile results in inducing larger overturning moments, leading to cause larger pile bending moments. When the inertial and kinematic loads act with a significant phase difference, the reduced horizontal pile accelerations will induce smaller pile bending moments, but the larger pile-cap rotations induced by higher phase difference between the two loads (see Garala and Madabhushi 2020) will further contribute to the pile bending in a single pile. In the case of pile groups, the overturning moment caused by inertial loads will be mainly resisted by axial pile compression and extension rather than pile bending (Mylonakis 1995), as shown in Fig. 17. This effect has been observed predominantly in the closely spaced pile group, with the piles of closely spaced pile group having smaller bending moments than single pile during all base excitations, irrespective of the phase difference between kinematic and inertial loads.

On the other hand, for the widely spaced pile group, the pile accelerations are smaller (see Fig. 10), but larger bending moments were observed in comparison to a closely spaced pile group (see Fig. 16). This can be due to the additional kinematic stresses imposed by the soil in between the widely spaced piles of pile group. This can also be justified with the piles in widely spaced pile group always have their peak bending moment at the interface of soil layers, whereas for the piles in closely spaced pile group, the peak bending moment occurs at the soil surface level during most base excitations (see Fig. 16). This indicates that the kinematic effects are predominant in a widely spaced pile group compared to a closely spaced pile group. Further, during BE5 excitation, the peak bending moment of widely spaced pile group is larger than the single pile as there is a significant phase difference between the kinematic and inertial loads in single pile but not in the widely spaced pile group (see Fig. 11). In most cases of conventional seismic pile design, it is usually assumed that a single pile will always attract higher accelerations and bending moments compared to a pile group. However, it has been seen in this study that this may not be true for all cases and the phase difference between the kinematic and inertial loads will critically governs this behaviour.

Moreover, similar to the kinematic pile bending moments, the shadowing effects in the presence of both kinematic and inertial loads are also different in the piles of closely spaced and widely spaced pile groups. In the closely spaced pile group, the pile-1 has larger bending moments than pile-3 at all depths of the pile foundation and during all excitations, as shown in Fig. 16. However, for the widely spaced pile group, the pile-1 has larger bending moments than pile-3 till to a depth ~1*d* beneath the interface and after that pile-3 has larger bending moments than pile-1. This difference is predominantly due to the kinematic loading effects as discussed in the earlier section. For pile groups under lateral loading conditions, Brown and Shie (1990), Ng et al. (2001) and Basile (2003), among others, reported that the shadowing effects will become less significant with the increase in pile spacing in pile groups. However, for piles under seismic loading conditions, though the pile-soil-pile interaction reduces with the increase in pile spacing, the group shadowing effects can still be predominant in widely spaced pile groups due to the significant kinematic loading effects.

Evaluation of Individual Contribution of Kinematic and Inertial loads

The importance of considering both kinematic and inertial loads in the seismic design of pile foundations has been clearly highlighted by the previous sections. However, the proportion of kinematic and inertial loads that needs to be considered in the seismic design of pile foundations is yet unclear. Either for pseudo-static or dynamic analyses, the combined effect of kinematic and inertial loads on the pile foundations can be expressed using Eq. (6) as:

$$F_T = (\beta \times F_I) + (\gamma \times F_K) \tag{6}$$

where F_T is the total seismic design load, F_I is the inertia load, F_K is the kinematic load, β and γ are the coefficients to combine F_I and F_K, respectively. As the contribution of kinematic and inertial loads varies with the time during an earthquake, the severest combination of β and γ should be considered for estimating the maximum F_T.

Based on pseudo-static analysis and dynamic finite element analysis, Abghari and Chai (1995) recommends that 25% of the peak inertial force should be combined with the peak kinematic displacement (i.e., β = 0.25 and γ = 1) while computing the peak pile deflection, whereas for computing the peak pile bending response, 50% of the peak inertial force should be combined with the peak kinematic displacement (i.e., β = 0.50 and γ = 1). Similarly, Tokimatsu et al. (2005) suggests that the sum of moments due to both inertial and kinematic effects should be considered as the maximum design moment when both the kinematic and inertial loads act in-phase with each other on the pile foundations. Alternatively, when the two-loads act against each other, the maximum moment should be determined by the square root of sum of the squares of the two forces (Tokimatsu et al. 2005). The recommendations of Tokimatsu et al. (2005) are based on observations from the dynamic centrifuge data and pseudo-static analysis. Further, a two-step design methodology has been proposed in the seismic design code for railway structures of Japan (RTRI 1999), as shown below (Murono and Nishimura 2000; Luo et al. 2002):

Step-1: Load combination with dominant inertial loads (β = 1), as shown in Eq. (7)

$$F_T = (1 \times F_I) + (\gamma \times F_K) \tag{7}$$

Step-2: Load combination with significant kinematic (soil deformation) loads (γ = 1), as shown in Eq. (8)

$$F_T = (\beta \times F_I) + (1 \times F_K) \tag{8}$$

The above two steps represent the extreme cases where only one of the two loads (either kinematic or inertial loads) is predominant. For all other intermediate cases, a suitable combination of β and γ values need to be considered for estimating F_T. Following Murono and Nishimura (2000), the values of β and γ can be determined using Eqs. 9a and 9b, respectively.

$$\beta = \frac{a(t_g)}{a_{max}} \tag{9a}$$

$$\gamma = \frac{\delta(t_a)}{\delta_{max}} \tag{9b}$$

where a is the inertial acceleration, δ is the soil surface deformation, t_g and t_a represent the time at which the soil surface deformation and acceleration of structure (inertial loads) attains a peak value δ_{max} and a_{max}, respectively.

To establish the relationship between the soil surface deformation and pile-cap acceleration, the pile accelerations from K+I flight are normalised with the corresponding absolute maximum pile acceleration (acc_{norm}, see Eq. 10a) and plotted against the normalised soil surface deformation (δ_{norm}, see Eq. 10b).

$$acc_{norm}(t) = \frac{a(t)}{|a_{max}|} \tag{10a}$$

$$\delta_{norm}(t) = \frac{\delta(t)}{|\delta_{\max}|} \tag{10b}$$

Fig. 18 shows the relationship between normalised pile acceleration and normalised soil surface deformation for all the tested pile foundations. In addition, Fig. 18 also shows the time instants at which the maximum soil surface deformation or maximum pile acceleration is occurred during each excitation.

As can be seen in Fig. 18, the plot between the normalised soil surface deformation and normalised pile acceleration will be an ellipse with negative slope (i.e., inclined by about 135°) when the kinematic and inertial loads act in the same direction on pile foundation (e.g., the response of single pile during BE3 excitation in Fig. 18). Contrarily, the ellipse will have positive slope, i.e., inclined by about 45°, when there is a significant phase difference between the kinematic and inertial loads (e.g., the response of single pile during BE2 and BE4 excitations in Fig. 18). When the kinematic and inertial loads act with a phase shift of nearly 90° on pile foundations, the area enclosed between the normalised soil surface deformation and normalised pile acceleration will be relatively larger (e.g., the response of widely spaced pile group during BE2 excitation in Fig. 18). These observations are in-line with the results of Murono and Nishimura (2000), though they expressed the phase relationship between the kinematic and inertial loads as a function of soil natural frequency (f_s) and natural frequency of soil-pile-structure system (f_{sps}).

Further, Murono and Nishimura (2000) provided the upper and lower limit curves for β and γ as a function of f_s/f_{sps} by performing extensive analytical studies using linear analysis. They also considered the case of super-structure yielding through non-linear analysis. Figs. 19(a and b) show the limits proposed by Murono and Nishimura (2000). In addition, Figs. 19(a and b) show the experimentally determined β and γ values from Fig. 18 and following Eqs. 9a and 9b. As Figs. 19(a and b) show, for most of the excitations, the β and γ values remain in between the upper limit of linear analysis and super-structure yielding case. This is to be expected as the linear analysis cannot be applicable for medium to large intensity excitations considered in this study. In addition, plotting β and γ values as a function of f_s/f_{sps} is resulting in different β and γ values for the similar f_s/f_{sps} ratio, as shown in Figs. 19(a and b). It is already shown in this study that the phase relationship between the kinematic and inertial loads can be expressed independent of the soil natural frequency (see Fig. 11). Therefore, the experimentally determined β and γ values are plotted as a function of f/f_{sps} (f is the driving frequency) along with the limits proposed by Murono and Nishimura (2000) and shown in Figs. 19(c and d). As Figs. 19(c and d) indicate, a better distribution of β and γ values can be seen compared to the distribution against f_s/f_{sps} (see Figs. 19(a and b). However, the β and γ values are still within the upper limit of linear analysis and yielding case for the considered medium to large intensity earthquakes. Therefore, there is a need to redefine the limits proposed by Murono and Nishimura (2000) for the non-linear cases, especially for the soil-pile-structure systems with f/f_{sps} >1. However, this requires an extensive parametric analysis by acquiring more data in addition to the data obtained from these series of centrifuge experiments.

Conclusions

A series of dynamic centrifuge experiments was performed at 60*g* on a model single pile and two 3×1 row pile groups with different pile spacing in a two-layered soil model to investigate the influence of pile spacing on the dynamic behaviour of pile groups. The soil models consisted of a soft clay underlain by a dense sand. The following are the major conclusions of the study:

- The pile group accelerations were relatively smaller in widely spaced pile group compared to a closely spaced pile group when both the pile groups respond at a similar normalised frequency (f/f_{sps}) ratio. This is probably due to the higher damping exhibited by the pile-soil-pile system of widely spaced pile group in comparison to closely spaced pile group.

- The kinematic pile bending moments in a single pile were always larger than the piles in a closely spaced pile group. This difference in peak kinematic pile bending moments between the single pile and piles of a closely spaced pile group increases with the increase in intensity of the earthquake. However, in a widely spaced pile group, the piles in the group can be subjected to kinematic bending moments close to that of a single pile indicating the reduction in pile-soil-pile interaction.
- In the presence of both kinematic and inertial loads, the peak pile bending moments will be larger for the piles in widely spaced pile group in comparison to the piles of closely spaced pile group. This is due to the significant kinematic stresses imposed by the soil between the piles in a widely spaced pile group. Further, the peak bending moment occurs close to the ground surface for the piles in closely spaced pile group during most excitations. However, for the widely spaced pile group, the peak bending moment occurs at the interface of soil layers, indicating the dominance of kinematic loads in the dynamic behaviour of widely spaced pile groups.
- Irrespective of the phase difference between kinematic and inertial loads, the bending moment in the piles of closely spaced pile group is always smaller than the bending moment of the single pile. However, the piles in widely spaced pile group can be subjected to bending moments larger than a single pile when there is a significant phase difference between the kinematic and inertial loads in single pile but not in the pile group.
- The proportion of kinematic and inertial loads that needs to be considered in the seismic analysis of pile foundations is not yet clear. There is a need to explore this aspect further, especially for the pile foundations in horizontal, non-liquefiable soil layers accounting the pile group and soil non-linearity effects during medium to large intensity earthquakes.

Data availability statement

Some or all data, models, or code that support the findings of this study are available from the corresponding author upon reasonable request.

Acknowledgements

The first author would also like to thank the Commonwealth Scholarship Commission (CSC) and Cambridge Trust for their doctoral scholarship. The authors extend their appreciation to the technicians at the Schofield Centre of Cambridge University for their assistance during the centrifuge experiments. The authors also appreciate the anonymous reviewers for constructive comments and suggestions, which greatly improved this article.

References

Abghari, A., and J. Chai. 1995. “Modeling of soil–pile–superstructure interaction for bridge foundations.” In *Proc., Performance of deep foundations under seismic loading,* 45-59. New York: ASCE.

Adachi, N., Y. Suzuki, and K. Miura. 2004. “Correlation Between Inertial Force and Subgrade Reaction of Pile in Liquefied Soil.” In *Proc*., *13th World Conference on Earthquake Engineering*, Vancouver, Canada.

Basile, F. 2003. *Numerical analysis and modelling in geomechanics: Analysis and design of pile groups*. Bull, J.W (Editor), Taylor and Francis Group, CRC Press, London.

Boulanger, R.W., C.J. Curras, B.L. Kutter, D.W. Wilson, and A. Abghari. 1999. “Seismic soil–pile–structure interaction experiments and analysis.” *Journal of Geotechnical and Geoenvironmental Engg.,* 125(9), 750–759.

Brennan, A.J., and S.P.G. Madabhushi. 2002. “Design and performance of a new deep model container for dynamic centrifuge testing.” In *Proc*., *International Conference on Physical Modelling in Geotechnics*, Balkema, Rotterdam, 183-188.

Brennan, A.J., N.I. Thusyanthan, and S.P.G. Madabhushi. 2005. “Evaluation of shear modulus and damping in dynamic centrifuge tests.” *Journal of Geotecnical. and Geoenviromental. Engineering*, 131(12), 1488–1498.

Brown, D. A., and C.F. Shie. 1990. “Numerical experiments into group effects on the response of piles to lateral loading.” *Computers and Geotechnics,* 10(3), 211-230.

BSI. 2015. BS 8004. *Code of practice for foundations*. *British Standards Institution*, London, UK.

Cai, Y.X., P.L. Gould, and C.S. Desai. 2000. “Nonlinear analysis of 3D seismic interaction of soil– pile–structure system and application.” *Engineering Structures,* 22(2), 191–199.

CEN (European Committee for Standardization) 2004. EN 1998-5: Eurocode 8: *Design of structures for earthquake resistance – part 5: Foundations, retaining structures and geotechnical aspects*, Brussels, Belgium: CEN European Committee for Standardization (CEN/TC250).

Chau, K.T., C.Y. Shen, and X. Guo. 2009. “Non-linear seismic soil-pile-structure interaction: shaking table tests and FEM analyses.” *Soil Dynamics and Earthquake Engineering*, 29, 300–310.

Darendeli, M.B. 2001. *Development of a new family of modulus reduction and material damping curves*. Ph.D. Dissertation, University of Texas Austin, USA.

Di Laora, R., A. Mandolini, and G. Mylonakis. 2012. “Insight on kinematic bending of flexible piles in layered soil.” *Soil Dynamics and Earthquake Engineering*, 43, 309-322.

Dobry, R., and M.J. O'Rourke. 1983. "Discussion of Seismic response of end-bearing piles" by Flores Berrones, R. & Whitman, R.V. *Journal of Geotechnical Engineering*, 109(5), 778-781.

Durante, M.G., L.D. Sarno, G. Mylonakis, C.A. Taylor, and A.L. Simonelli. 2016. "Soil–pile–structure interaction: experimental outcomes from shaking table tests." *Earthquake Engineering and Structural Dynamics*, 45, 1041–1061.

Fan, K., G. Gazetas, A. Kaynia, and E. Kausal. 1991. "Kinematic seismic response of single piles and pile groups." *Journal of Geotechnical Engineering*, 117(12), 1860–1879.

Garala, T.K. 2020. *Seismic response of pile foundations in soft clays and layered soils.* Ph.D. Dissertation, University of Cambridge, UK.

Garala, T. K., and S.P.G. Madabhushi. 2019. "Seismic behaviour of soft clay and its influence on the response of friction pile foundations." *Bulletin of Earthquake Engineering*, 17(4), 1919–1939.

Garala, T.K., and S.P.G. Madabhushi. 2020. "Influence of the phase difference between kinematic and inertial loads on seismic behaviour of pile foundations embedded in layered soils." *Canadian Geotechnical Journal*. https://doi.org/10.1139/cgj-2019-0547.

Garala, T.K., S.P.G. Madabhushi, and R. Di Laora. 2020. "Experimental investigation of kinematic pile bending in layered soils using dynamic centrifuge modelling." *Géotechnique*. https://doi.org/10.1680/jgeot.19.p.185.

Gazetas, G., T. Tazoh, K. Shimizu, and K. Fan. 1993. "Seismic response of the pile foundation of Ohba-Ohashi Bridge." In *Proc., 3rd International conference on Case Histories in Geotechnical Engineering,* Missouri, 1803-1809.

Ghosh, B., and S.P.G. Madabhushi. 2002. "An efficient tool for measuring shear wave velocity in the centrifuge." In *Proc., International Conference on Physical Modelling in Geotechnics,* Balkema, Rotterdam, 119–124.

Hardin, B.O., and V.P. Drnevich. 1972. "Shear modulus and damping in soils: Design equation and curves." *Journal of Soil Mechanics and Foundation Engineering Division*, 98(SM7), 667-692.

Hashash, Y.M.A., M.I. Musgrove, J.A. Harmon, I. Okan, D.R. Groholski, C.A. Philipis, and D. Park. 2017. *DEEPSOIL 7.0*, User Manual, University of Illinois at Urbana-Champaign, USA.

Hokmabadi, A.S. 2014. *Effect of dynamic soil–pile–structure interaction on seismic response of mid-rise moment resisting frames*. PhD Dissertation, University of Technology Sydney, Australia.

Hussien, M.N., T. Tobita, S. Iai, and M. Karray. 2016. "Soil-pile-structure kinematic and inertial interaction observed in geotechnical centrifuge experiments." *Soil Dynamics and Earthquake Engineering*, 89, 75-84.

Kampitsis, A.E., E.J. Sapountzakis, S.K. Giannakos, and N.A. Gerolymos. 2013. "Seismic soil pile- structure kinematic and inertial interaction – A new beam approach." *Soil Dyn. Earthquake Engineering*, 55, 211–224.

Kavvadas, M., and G. Gazetas. 1993. "Kinematic seismic response and bending of free-head piles in layered soil." *Geotechnique*, 43(2), 207-222.

Ke, W., Q. Liu, and C. Zhang. 2019. "Kinematic bending of single piles in layered soil." *Acta Geotechnica*, 14, 101–110.

Luo, C., X. Yang, C. Zhan, X. Jin, and Z. Ding. 2016. "Nonlinear 3D finite element analysis of soil – pile – structure interaction system subjected to horizontal earthquake excitation." *Soil Dyn. Earthq. Eng.*, 84, 145–156.

Luo, X., Y. Murono and A. Nishimura. 2002. "Verifying adequacy of the seismic deformation method by using real examples of earthquake damage". *Soil Dynamics and Earthquake Engineering,* 22(1), 17–28.

Madabhushi, S.P.G. 2014. *Centrifuge modelling for civil engineers*. CRC Press, Taylor and Francis Group, Florida.

Madabhushi, S.P.G., J. Knappett, and S.K. Haigh. 2010. *Design of pile foundations in liquefiable soils*. Imperial college press, London.

Madabhushi, S.P.G., S.K. Haigh, N.E. Houghton, and E. Gould. 2012. "Development of a servo-hydraulic earthquake actuator for the Cambridge Turner beam centrifuge." *International Journal of Physical Modelling in Geotechnics,* 12(2), 77-88.

Maheshwari, B.K., K.Z. Truman, M.H. El Naggar, and P.L. Gould. 2004. "Three-dimensional finite element nonlinear dynamic analysis of pile groups for lateral transient and seismic excitations." *Canadian Geotechnical Journal*, 41, 118–33.

Maiorano, R.M.S., L. de Sanctis, S. Aversa, and A. Mandolini. 2009. "Kinematic response analysis of piled foundations under seismic excitations." *Canadian Geotechnical Journal,* 46(5), 571-584.

Margason, E., and D.M. Halloway. 1977. "Pile bending during earthquakes." In Vol. II of *Proc*., *Sixth World Conference on Earthquake Engineering,* Meerut, India, 1690-1696.

Meymand, P.J. 1998. *Shaking table scale model tests of nonlinear soil-pile-superstructure interaction in soft clay*. PhD Dissertation, University of California, Berkeley, USA.

Mizuno, H. 1985. Pile damage during earthquakes in Japan (1923-1983). "Dynamic response of pile foundations – Experiment, analysis and observation." *ASCE Geotechnical Publication*, 11, 53-78.

Murono, Y. and A. Nishimura. 2000. "Evaluation of seismic force of pile foundation induced by inertial and kinematic interaction." In *Proc., 12th World Conference on Earthquake Engineering*, Auckland, New Zealand.

Mylonakis G, Nikolaou A, Gazetas G. 1997. "Soil-pile-bridge seismic interaction: kinematic and inertial effects. Part I: soft soil." *Earthquake engineering and structural dynamics*, 26, 337–359.

Mylonakis, G. 1995. *Contributions to static and seismic analysis of piles and pile-supported bridge piers*. PhD dissertation, State University of New York at Buffalo, USA.

Mylonakis, G. 2001. "Simplified method for seismic pile bending at soil-layer interfaces." *Soils and Foundations*, 41(4), 47-58.

Ng, C.W.W., L. Zhang, and D.C.N. Nip. 2001. "Response of laterally loaded large-diameter bored pile groups." *Journal of Geotechnical and Geoenvironmental Engineering*, 127(8), 658-669.

Nikolaou, S., G. Mylonakis, G. Gazetas, and T. Tazoh. 2001. "Kinematic pile bending during earthquakes: analysis and field measurements." *Géotechnique*, 51(5), 425-440.

Oztoprak, S., and M.D. Bolton. 2013. "Stiffness of sand through a laboratory test database." *Géotechnique*, 63(1), 54-70.

Pitilakis, D., M. Dietz, D.M. Wood, D. Clouteau, and A. Modaressi. 2008. "Numerical simulation of dynamic soil–structure interaction in shaking table testing." *Soil Dynamics and Earthquake Engineering*, 28, 453–467.

Rahmani, A., M. Taiebat, W.D.L. Finn, C.E. Ventura. 2018. "Evaluation of p-y springs for nonlinear static and seismic soil-pile interaction analysis under lateral loading." *Soil Dyn. Earthquake Engineering*, 115, 438–447.

Railway Technical Research Institute (RTRI). 1999. *Seismic design code for railway structures*. Maruzen, Tokyo (in Japanese)

Rollins, K.M., R.J. Olsen, J.J. Egbert, D.H. Jensen, K.G. Olsen, and B.H. Garrett. 2006. “Pile spacing effects on lateral pile group behaviour: load tests.” *Journal of Geotech. and Geoenvironmental Engng*, 132 (10), 1262-1271.

Rovithis, E., E. Kirtas, and K. Pitilakis. 2009. “Experimental p-y loops for estimating seismic soil-pile interaction.” *Bulletin of Earthquake Engineering*, 7(3), 719–736.

Schofield, A.N. 1980. “Cambridge geotechnical centrifuge operations.” *Géotechnique*, 30(3), 227–268.

Shirato, M., Y. Nonomura, J. Fukui, S. Nakatani. 2008. “Large-Scale Shake Table Experiment and Numerical Simulation on the Nonlinear Behavior of Pile-Groups Subjected to Large-Scale Earthquakes.” *Soils and Foundations*, 48(3), 375-396.

Sica, S., G. Mylonakis, A.L. Simonelli. 2011. “Transient kinematic pile bending in two-layer soil.” *Soil Dynamics and Earthquake Engineering*, 31, 891–905.

Teymur, B., and S.P.G. Madabhushi. 2003. “Experimental study of boundary effects in dynamic centrifuge modelling.” *Geotechnique*, 53(7), 655-663.

Tokimatsu, K., H. Suzuki, and M. Sato. 2005. “Effects of inertial and kinematic interaction on seismic behaviour of pile with embedded foundation.” *Soil Dynamics and Earthquake Engineering*, 25, 753-762.

Viggiani, G., and J.H. Atkinson. 1995. “Stiffness of fine-grained soil at very small strains.” *Géotechnique*, 45(2), 249-265.

Wang, R., X. Liu, and J.M. Zhang. 2017. “Numerical analysis of the seismic inertial and kinematic effects on pile bending moment in liquefiable soils.” *Acta Geotechnica*, 12, 773-791.

Wilson, D. 1998. *Dynamic Centrifuge Tests of Pile Supported Structures in Liquefiable Sand*. Ph.D. Dissertation, University of California, Davis, USA.

Yoo, M.T., J.T. Han, J.I. Choi, and S.Y. Kwon. 2017. “Development of predicting method for dynamic pile behaviour by using centrifuge tests considering the kinematic load effect.” *Bulletin of Earthquake Engineering*, 15, 967-989.

List of Tables

Table 1. Existing literature on the phase relationship between the seismic kinematic and inertial loads on pile foundations

Study	**Method**	**Soil**	**Foundations**	**In-phase condition**	**Out-of-phase condition**
Murono and Nishimura (2000)	Analytical study based on beam on linear/non-linear Winkler foundation	Soft soil	Pile-supported railroad bridge	$T_g > T_s$	$T_g < T_s$
Adachi et al. (2004)	1*g* shaking table tests	Liquefiable saturated sands	3×3 pile group made of acrylic tubes	$T_g < T_s$	$T_g > T_s$
Tokimatsu et al. (2005)	Large 1*g* shaking table tests	Dry and liquefiable saturated sands	2×2 steel pile group	$T_g > T_s$	$T_g < T_s$
Yoo et al. (2017)	Dynamic centrifuge tests	Dry and liquefiable saturated sands	Single pile	Always out-of-phase irrespective of ground conditions	
Garala & Madabhushi (2020)	Dynamic centrifuge tests	Two-layered non-liquefiable soils	Single pile and 1×3 row pile group	$f < f_{sps}$	$f > f_{sps}$

* T_g and T_s are the fundamental periods of the ground and superstructure, respectively; f is the excitation frequency; f_{sps} is the strain dependent fundamental frequency of the soil-pile-structure system.

Table 2. Shear strains determined at the interface of soil layers following Brennan et al. (2005) in Test-FPC

Excitation	Frequency (Hz)	Peak base acceleration (g)	Test-FPC (K flight)		
			Top of sand layer (%)	Bottom of clay layer (%)	Clay to sand ratio
BE1	0.667 Hz	0.045	0.03	0.048	1.6
BE2	1.167 Hz	0.087	0.09	0.38	4.22
BE3	0.667 Hz	0.174	0.21	0.5	2.38
BE4	0.833 Hz	0.193	0.3	1.18	3.9

Table 3. Shear strains determined at the interface of soil layers following Brennan et al. (2005) in Test-FPW

Excitation	Frequency (Hz)	Peak base acceleration (g)	Test-FPW (K flight)		
			Top of sand layer (%)	Bottom of clay layer (%)	Clay to sand ratio
BE1	0.667 Hz	0.045	0.05	0.08	1.6
BE2	1.167 Hz	0.088	0.046	0.44	9.56
BE3	0.667 Hz	0.176	0.19	0.48	2.53
BE4	0.833 Hz	0.20	0.16	0.87	5.44

List of Figures

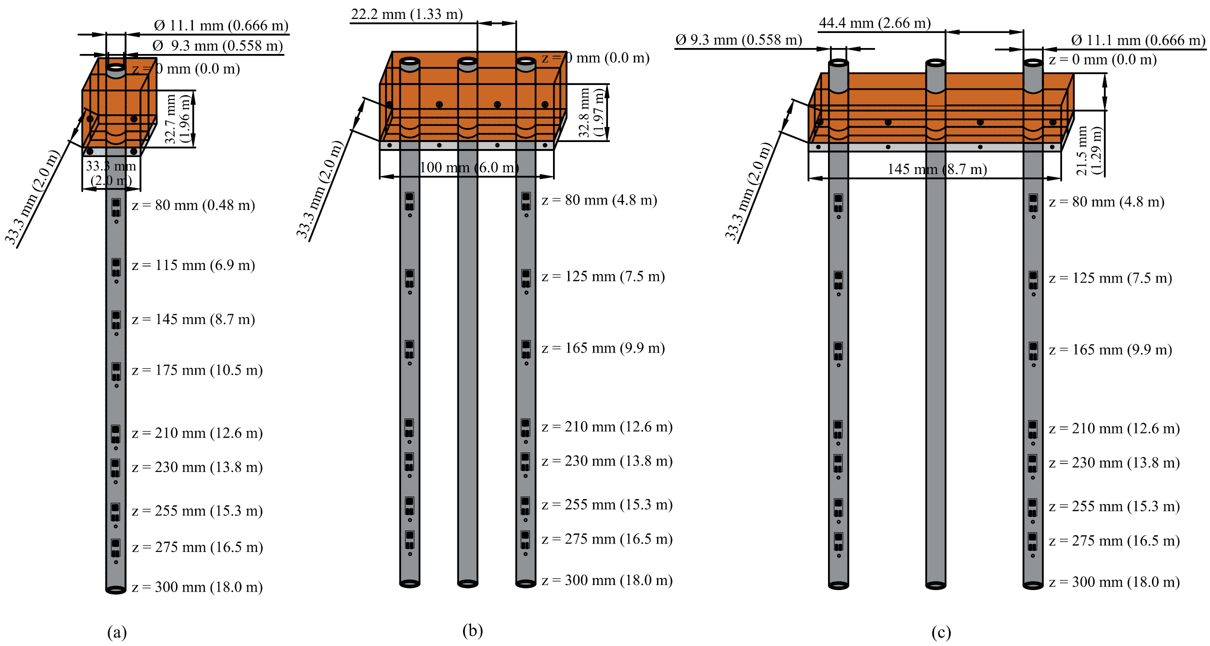

Fig. 1. Schematic view of the pile foundations tested (a) single pile (SP) (b) closely spaced pile group (CPG) and (c) widely spaced pile group (WPG).

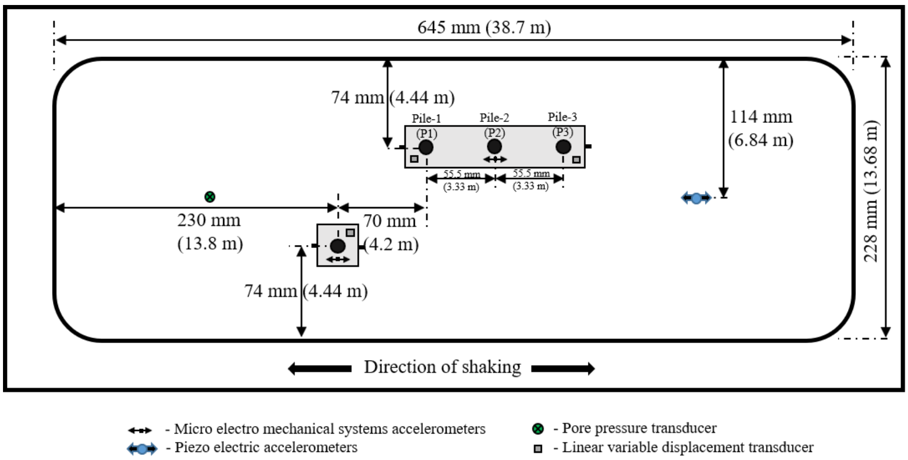

Fig. 2. Plan view of the centrifuge model in Test-FPW.

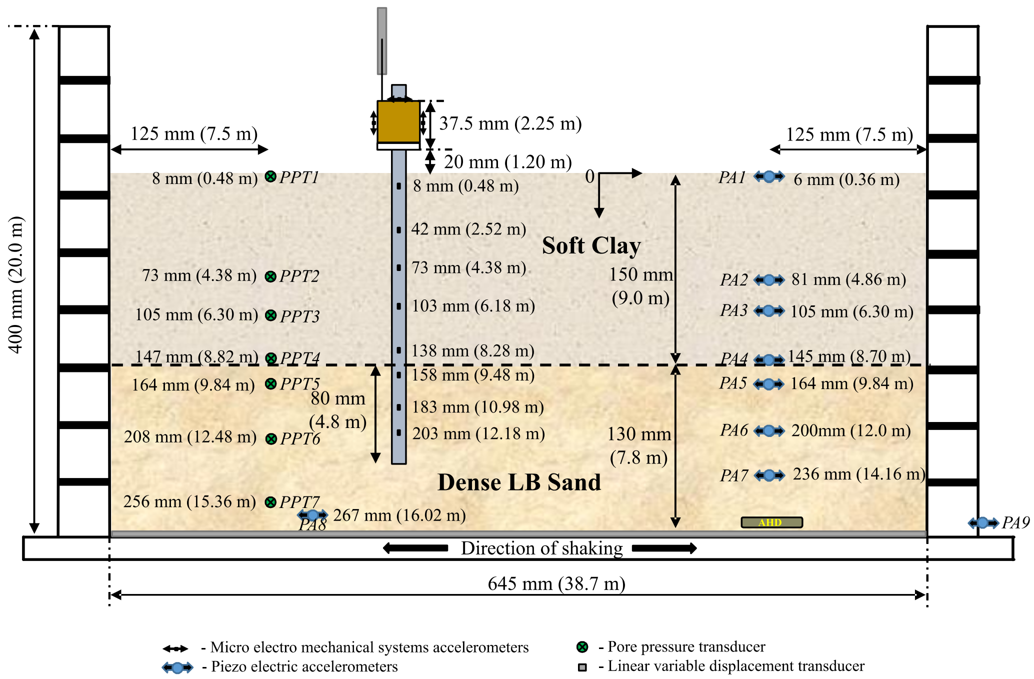

Fig. 3. Elevation of the centrifuge model in Test-FPW.

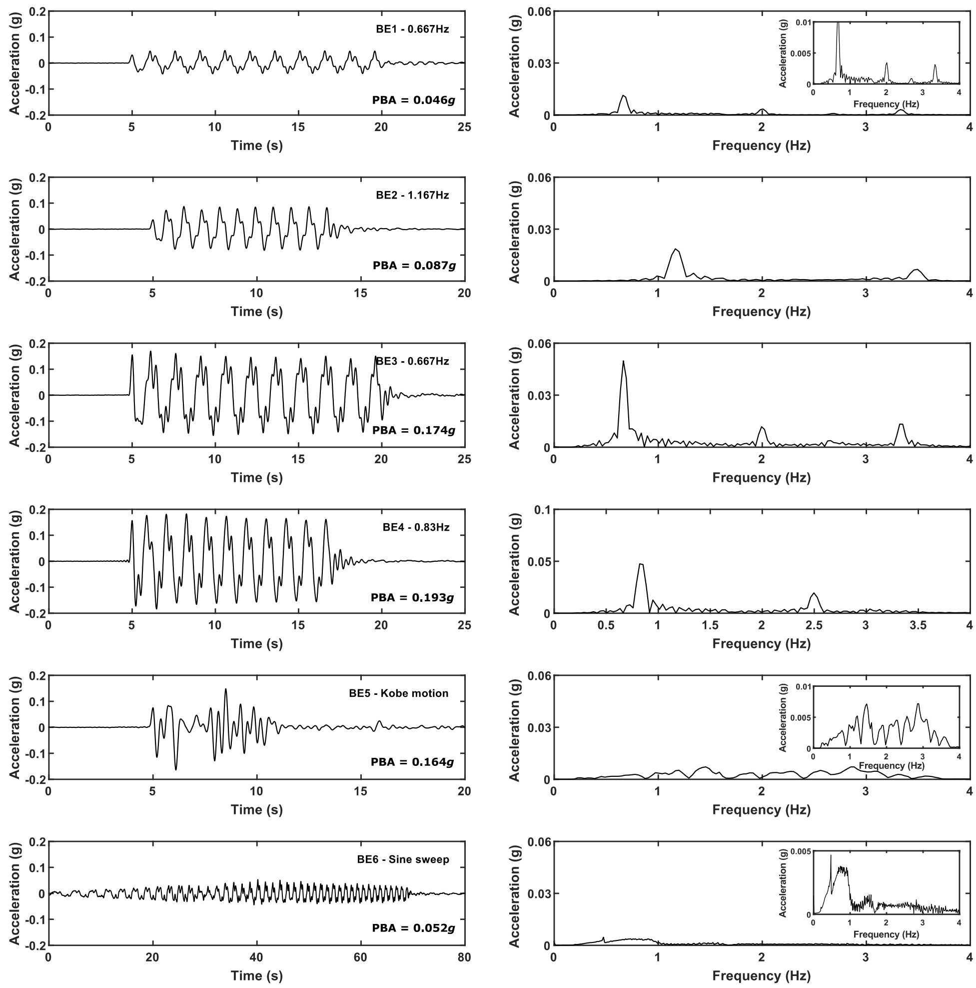

Fig. 4. Prototype base excitations considered in the study (PBA refers to peak base acceleration).

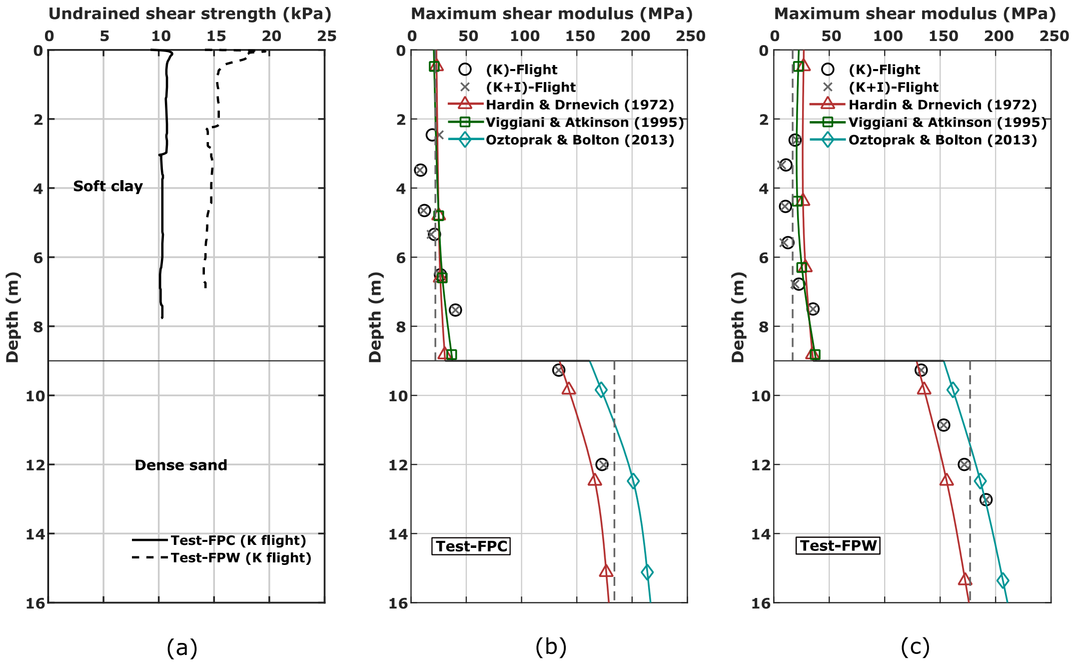

Fig. 5. (a) Undrained shear strength of the clay layers, (b) and (c) maximum shear modulus of soil layers in Test-FPC and Test-FPW, respectively.

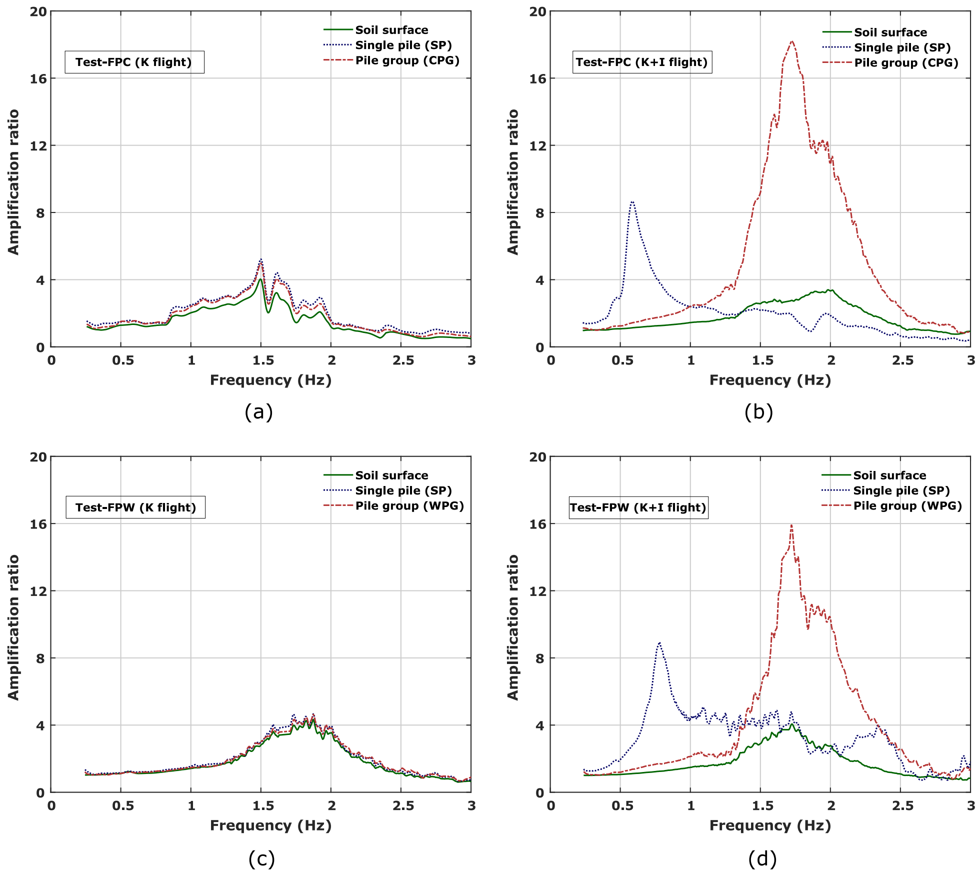

Fig. 6. Variation of amplification ratio against frequency for soil strata and pile foundations in both flights of two centrifuge tests.

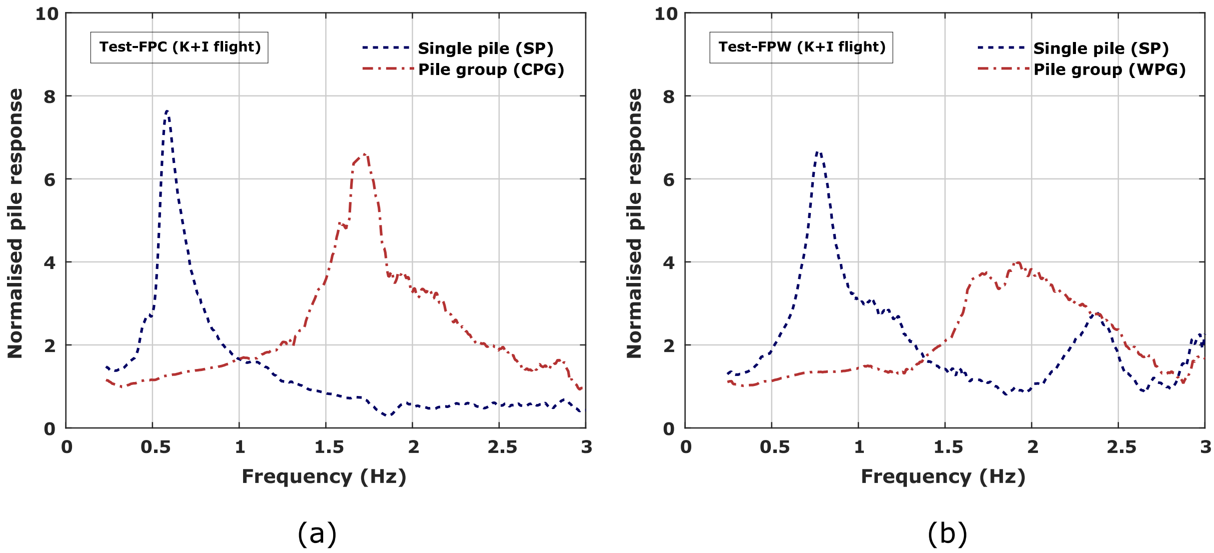

Fig. 7. Normalised acceleration response of pile foundations in K+I flight during (a) Test-FPC and (b) Test-FPW.

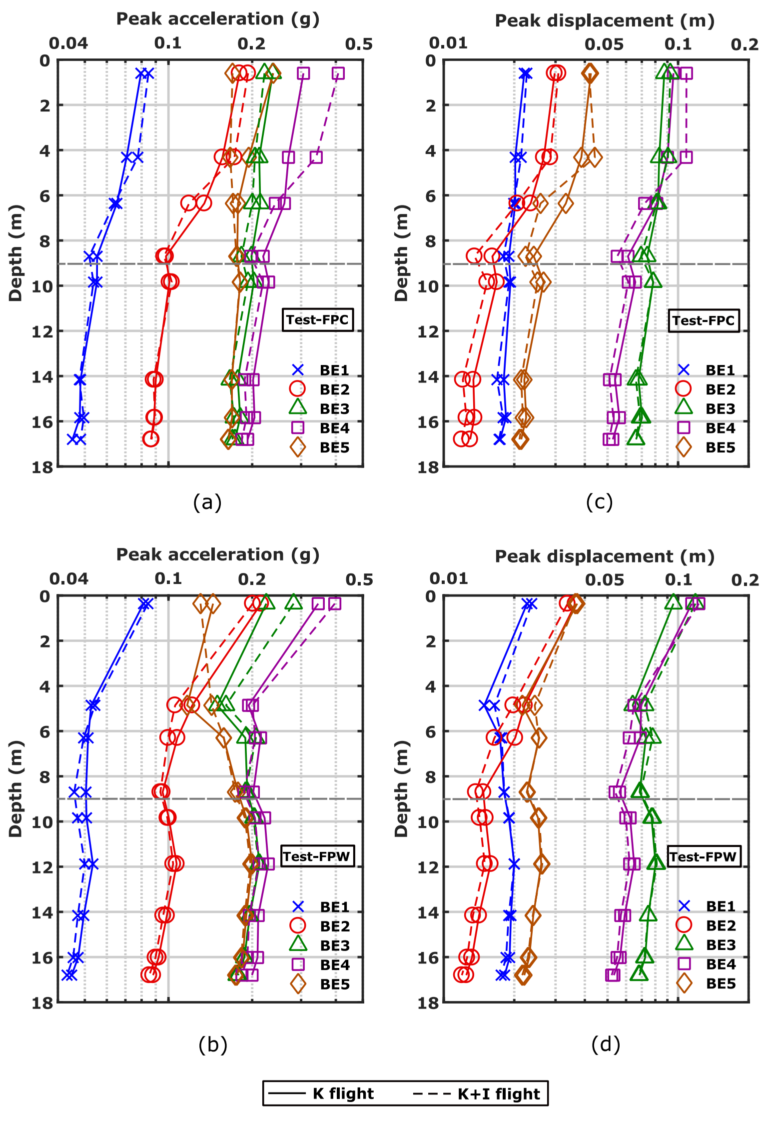

Fig. 8. Dynamic response of soil strata for various base excitations in Test-FPC and Test-FPW.

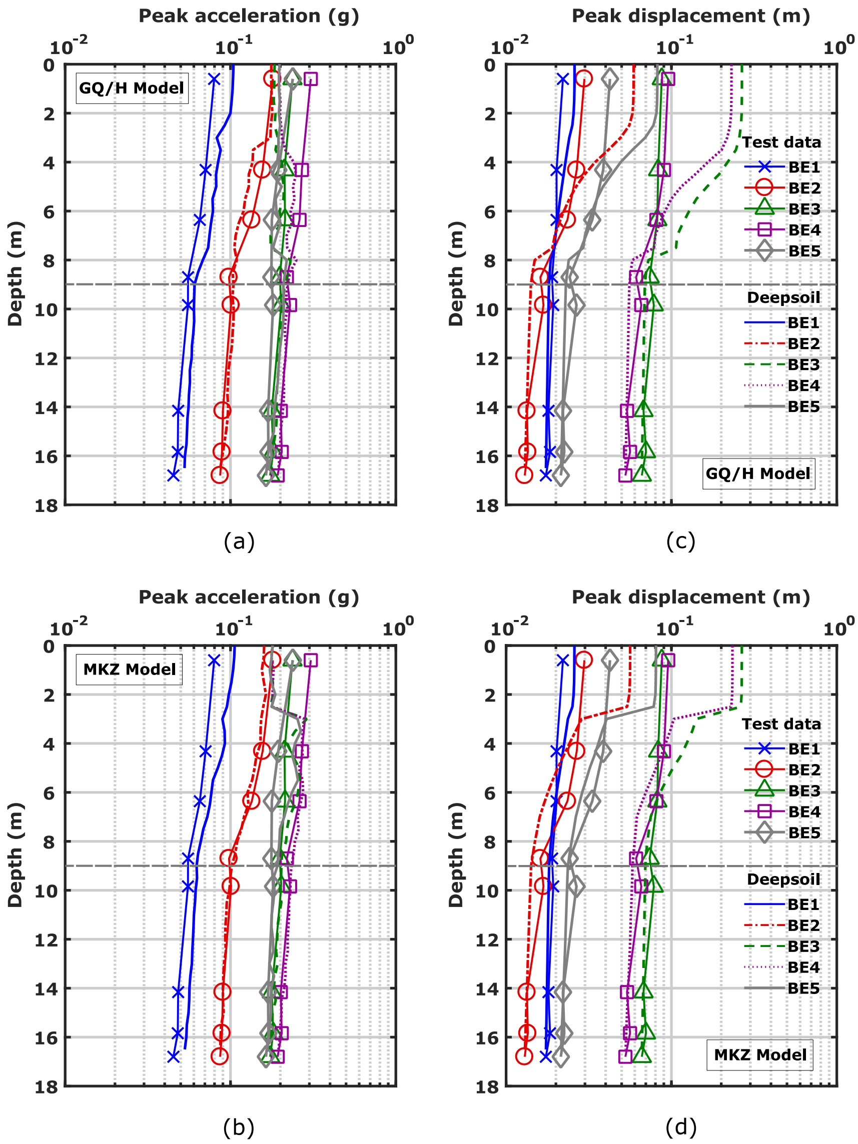

Fig. 9. Comparison of dynamic response of soil strata from centrifuge tests and DEEPSOIL analyses.

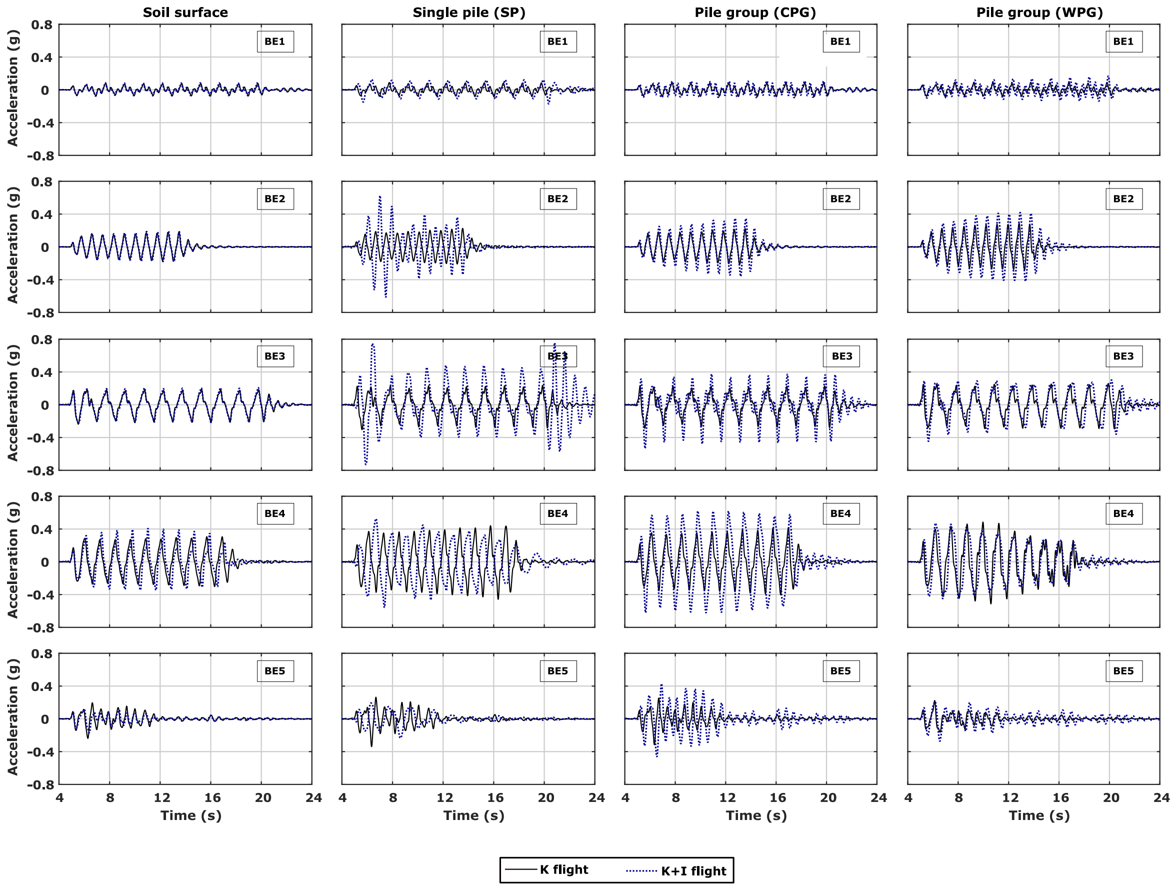

Fig. 10. Acceleration time histories of soil surface and tested pile foundations in both flights of two centrifuge tests.

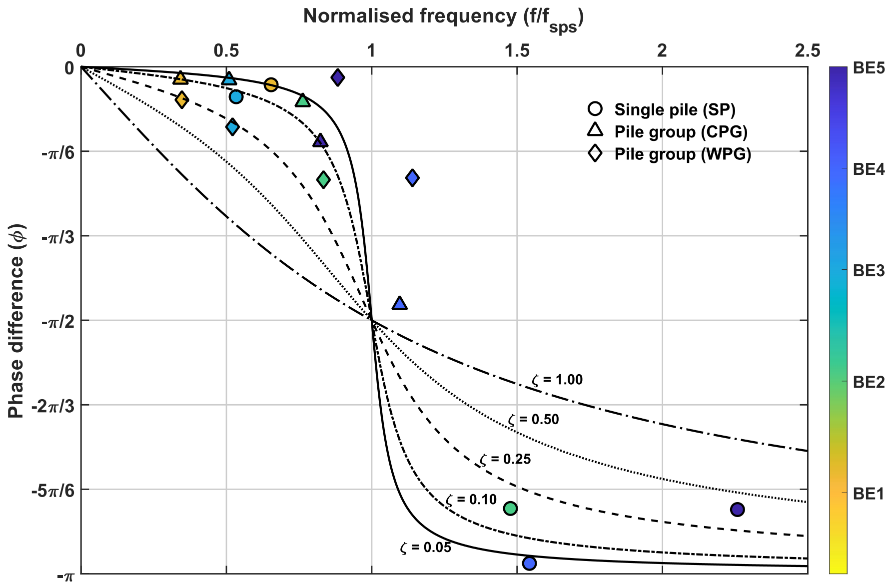

Fig. 11. Values of experimentally determined phase difference between the kinematic and inertial loads on conventional phase variation between the force and displacement of a viscously damped linear second-order system subjected to a harmonic response.

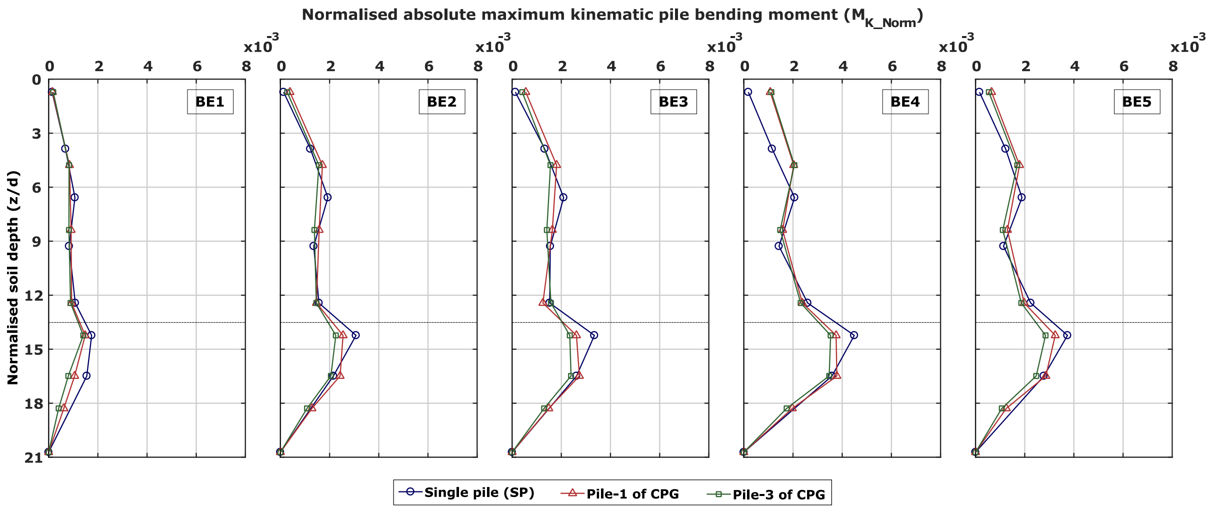

Fig. 12. Normalised absolute maximum kinematic pile bending moments of single pile and closely spaced pile group from Test-FPC.

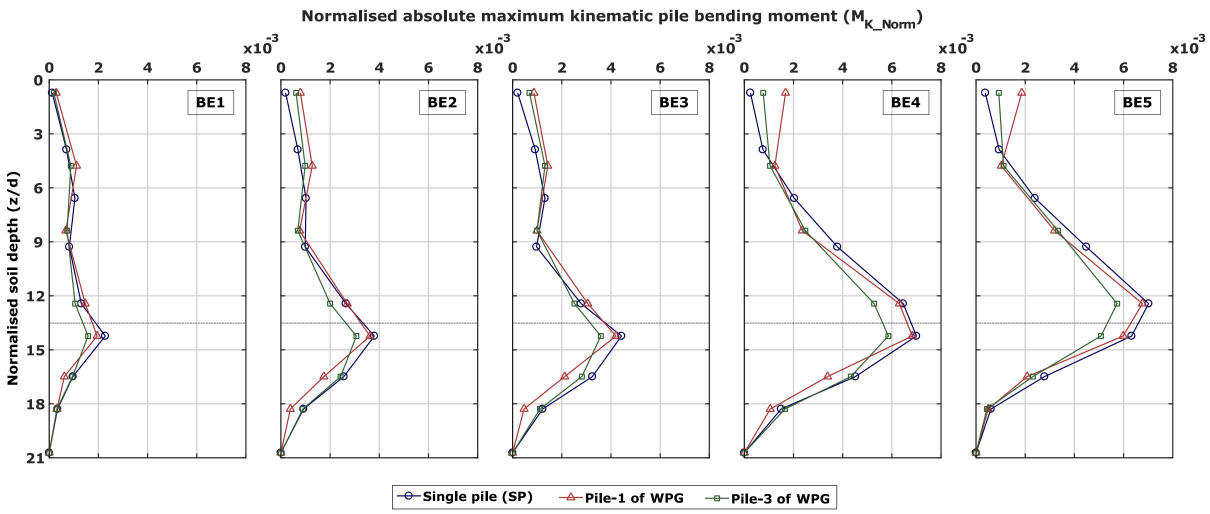

Fig. 13. Normalised absolute maximum kinematic pile bending moments of single pile and widely spaced pile group from Test-FPW.

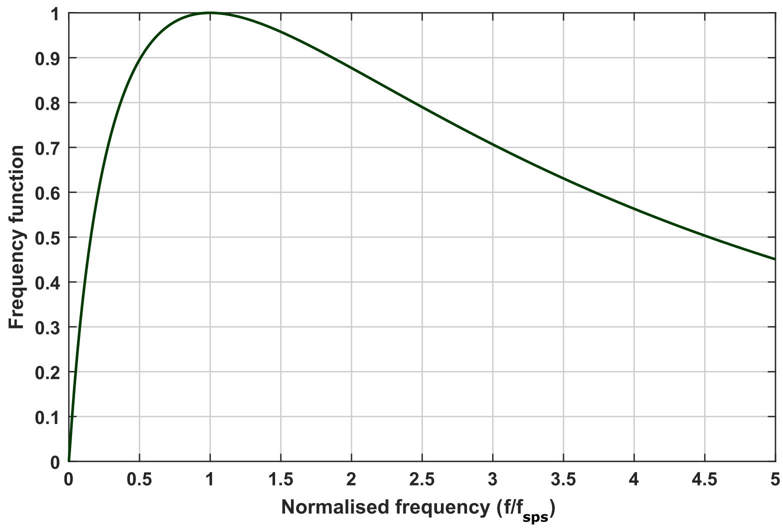

Fig. 14. Frequency normalisation function used to normalise the pile bending moments in K+I flight.

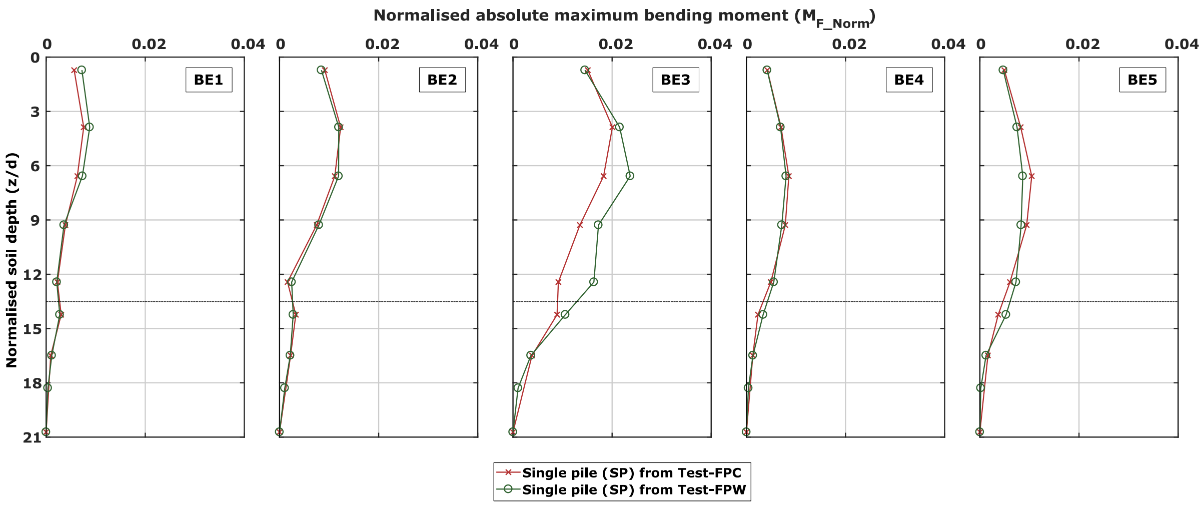

Fig. 15. Comparison of single pile bending response from two different tests with the proposed bending moment normalisation.

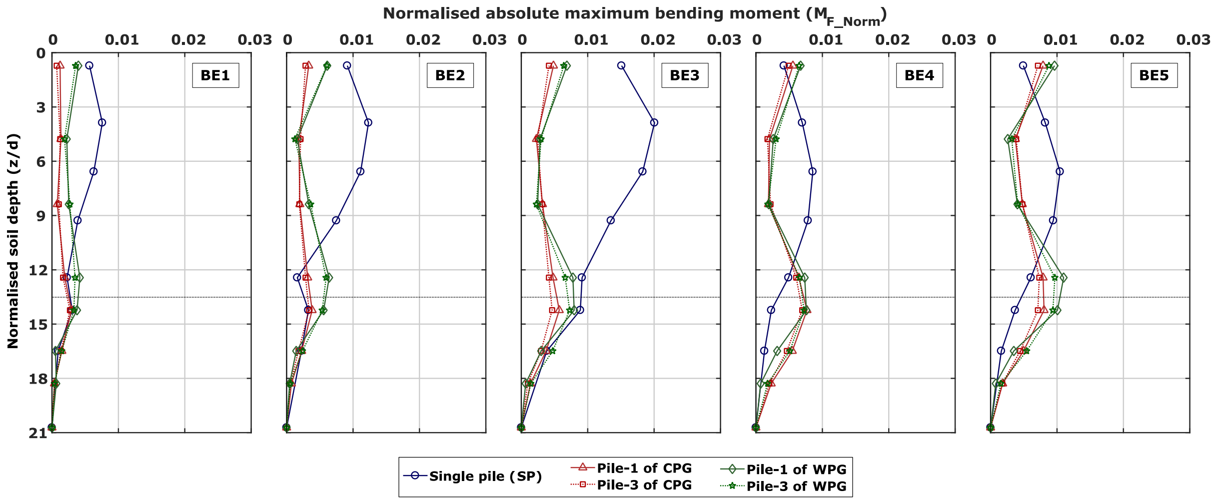

Fig. 16. Comparison of normalised absolute maximum bending moments of single pile and end piles of the pile groups in K+I flight.

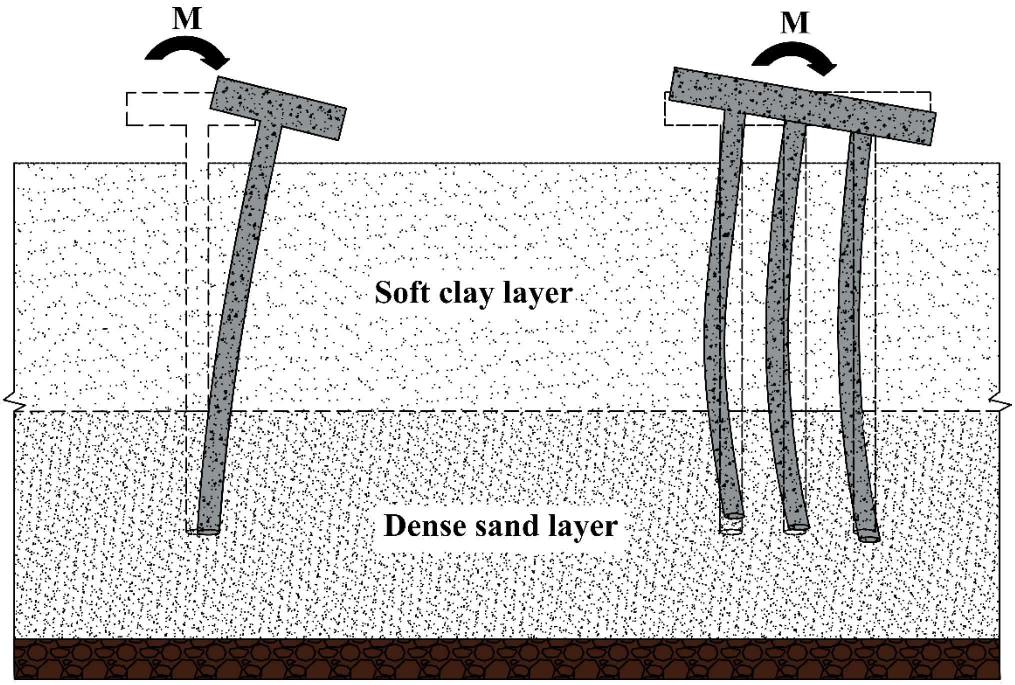

Fig. 17. Influence of over-turning moments on a single pile and pile group (at an exaggerated scale).

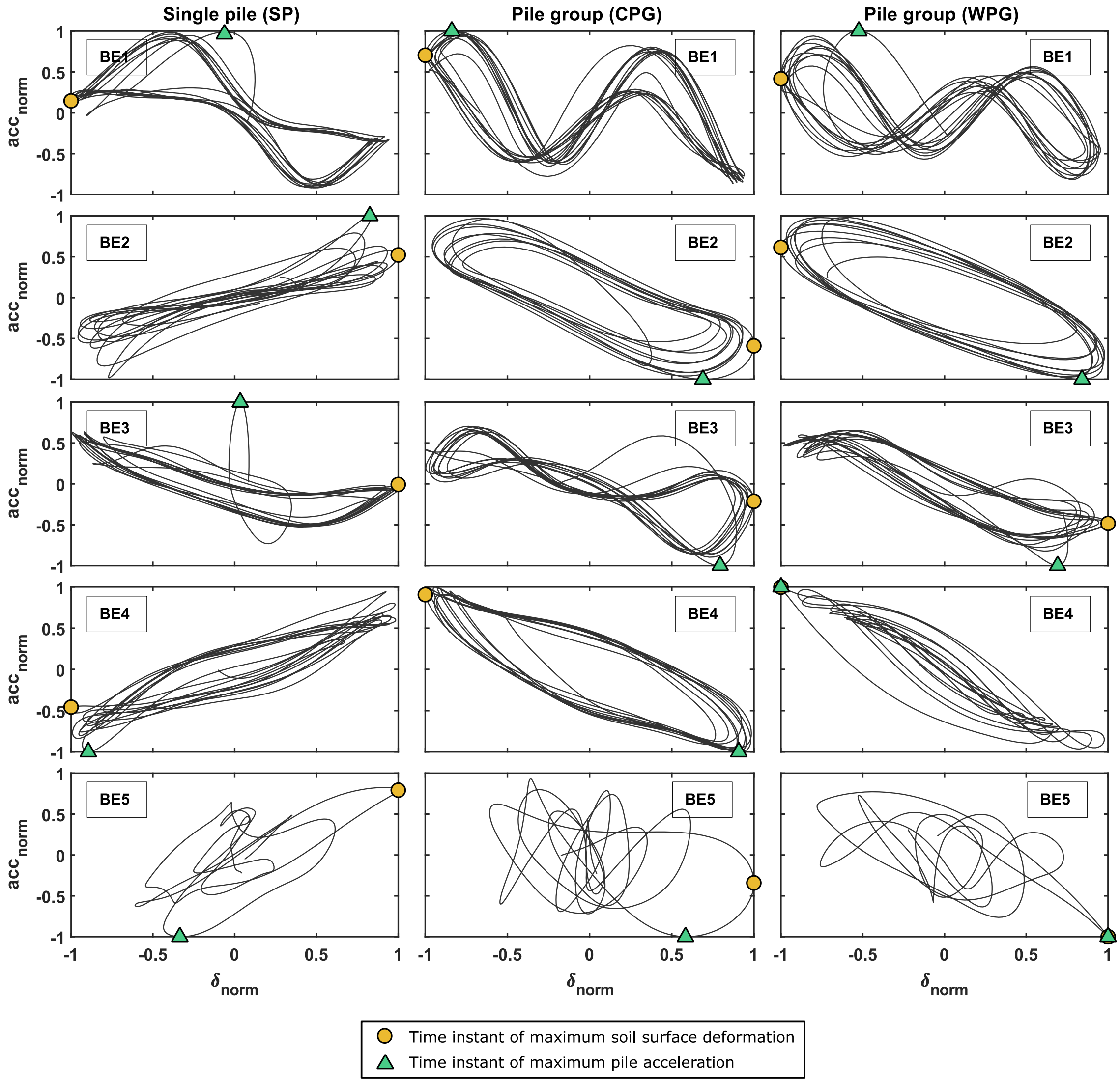

Fig. 18. Relationship between the normalised pile acceleration and normalised soil surface deformation along with the time instants of maximum soil surface deformation and pile acceleration.

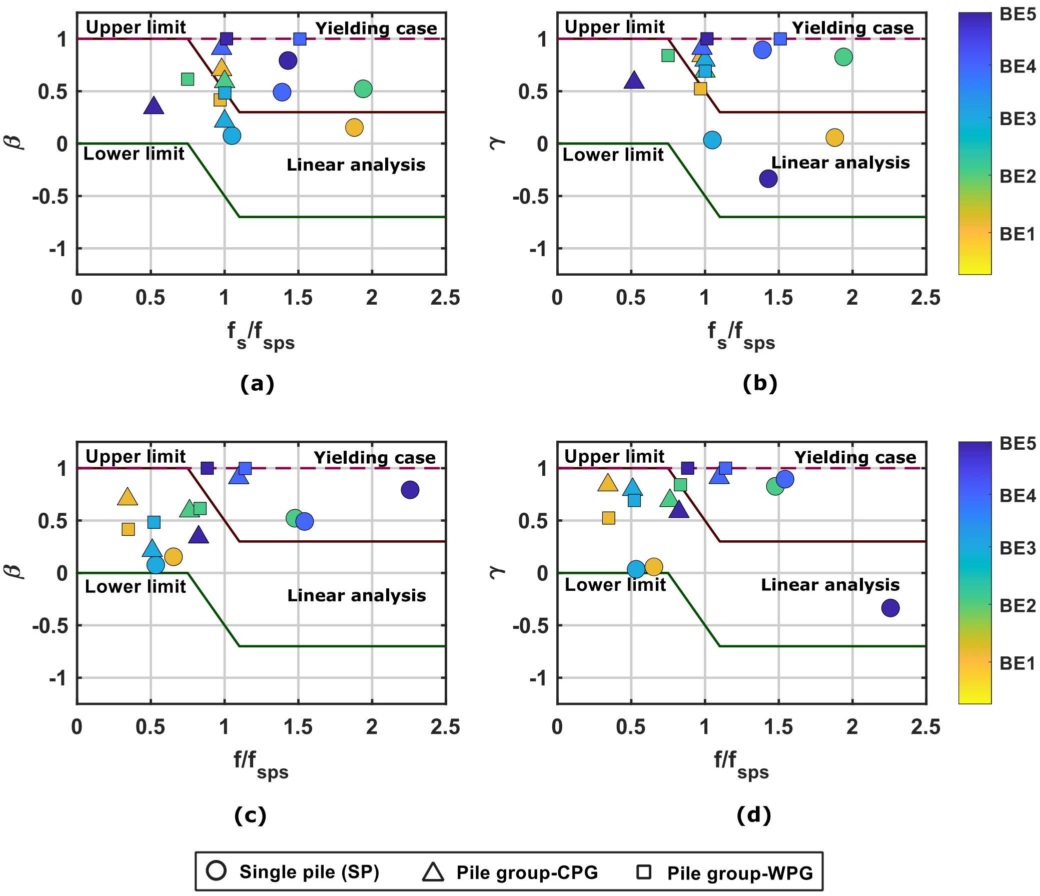

Fig. 19. Values of coefficients β and γ: (a) and (b) as a function of f_s/f_{sps} as suggested by Murono and Nishimura (2000), and (c) and (d) as a function of f/f_{sps} as proposed in this study.